DIRECT MEASUREMENT OF WATER AND SOLUTE MASS FLUXES USING A PASSIVE SURFACE WATER FLUX METER

By

JULIE C. PADOWSKI

A THESIS PRESENTED TO THE GRADUATE SCHOOL
OF THE UNIVERSITY OF FLORIDA IN PARTIAL FULFILLMENT
OF THE REQUIREMENTS FOR THE DEGREE OF
MASTER OF SCIENCE

UNIVERSITY OF FLORIDA

2005

Copyright 2005

by

Julie C. Padowski

This thesis is dedicated to my siblings, Jeannie and Nick, who have also chosen the path of higher learning. Good luck.

ACKNOWLEDGMENTS

I would especially like to thank my major advisor, Dr. James W. Jawitz, for all the time, effort and patience he invested in me and my work, and my committee members Dr. Kirk Hatfield and Dr. Michael Annable for their advice and support.

I sincerely appreciate the expertise and humor of Dr. Jaeyhun Cho and his many hours of laboratory assistance, as well as the guidance I received from Dr. Mark Newman and Dr. Huaguo Wang. I would also like to thank the employees of the Coastal Engineering Laboratory for access to their equipment.

I am especially grateful for the help and support of my fellow graduate students, D. Perkins, J. Bhadha, W. Ha, E. Atkinson. In particular, I would like to thank A. Olsen for the invaluable scholarly wisdom he imparted on me during all the hours he hovered annoyingly behind my desk and M.K. Hamilton for all her wonderful emotional support. Special thanks go to all the friends I have met here, especially S. Anderson, S. Curtis, and S. Muller and to my parents and siblings for keeping me positive and focused with their support and encouragement.

TABLE OF CONTENTS

LIST OF TABLES

LIST OF FIGURES

Abstract of Thesis Presented to the Graduate School
of the University of Florida in Partial Fulfillment of the
Requirements for the Degree of Master of Science

DIRECT MEASUREMENT OF WATER AND SOLUTE MASS FLUXES USING A PASSIVE SURFACE WATER FLUX METER

By

Julie C. Padowski

December 2005

Chair: James W. Jawitz
Cochair: Kirk Hatfield
Major Department: Soil and Water Science

Current methods for determining pollutant loads typically involve collecting separate instantaneous measurements of water velocities and solute concentrations at discrete points in space and time. The data must be combined, interpolated and integrated after collection in order to estimate local water and solute fluxes in streams. The frequency with which these parameters are measured typically depends upon the availability of resources (time, money, manpower, etc.) and often leads to under-sampling.

A method is presented here for direct measurement of surface water flux (velocity) and solute mass flux using a Passive Surface Water Flux Meter (PSFM). The PSFM integrates instantaneous measurements of water velocity and solute concentration to yield a direct measurement of time-averaged water and solute mass fluxes. The shape of the PSFM profile determines the velocity distribution around a submerged device,

creating a pressure gradient across two known points. A permeable, sorptive cartridge is attached between these points, and fluxes are measured by simultaneously sorbing contaminants while eluting a resident tracer from this cartridge. Analysis of the cartridge reveals the relative amount of resident tracer lost and mass of contaminant sorbed, which is then used to calculate water and solute fluxes.

Several combinations of PSFM bodies and cartridges were tested to validate the theoretical equations for water and solute flux. Flume laboratory trials were performed under steady state and transient flow conditions. A cylindrical and a hydrofoil-shaped PSFM were tested with two different tracers: a visible, non-reactive dye and a non-visible ethanol tracer. Experiments showed that both PSFM shapes produced a sufficient pressure gradient for flow through the cartridge to occur. The non-reactive dye and the ethanol tracers predicted water velocities within 8% and 26% of the true stream velocity under steady-state conditions, respectively. True vs. ethanol-estimated solute fluxes differed by 28% when measuring solute mass flux under the same conditions. Transient solute flux experiments were inconclusive.

Results showed that the theoretical concepts of the PSFM were validated in steady-state flow conditions using both the cylindrical and hydrofoil-shaped PSFMs. The PSFM shape did not affect measurement accuracy under the velocity ranges tested, however, the type of cartridge used did affect how precisely flux was measured in the flume. In conclusion, this preliminary study suggests that with further cartridge development the theoretical model of the PSFM could be used to accurately predict water and solute fluxes and holds promise for measuring pollutant loads in natural systems.

CHAPTER 1
INTRODUCTION

1.1 Background

The impact of human activities on local and regional ecosystems has become a global concern over the last several decades. Although anthropogenic processes have been affecting overall environmental quality for millennia, it is within the past century that noticeable changes have taken place, especially in terms of water quality degradation (Meybeck and Helmer, 1989). The health of watersheds across the globe have been rapidly deteriorating under the pressures of expanding human populations, industrial and agricultural growth and other socio-economic factors (Meybeck and Helmer, 1989; Carpenter et. al, 1998; Parry, 1998). This deterioration is commonly referred to as "pollution" and can have long-ranging effects, both through space and time.

Water quality monitoring programs were established by the late 1800's to identify and quantify factors that lead to the degradation of water quality. Since then, a list of over 100 descriptors have been recognized due to advances in sampling and analyzing techniques, including dissolved oxygen, pH, temperature, total suspended solids (TSS), bacteria, metals, nutrients, organic matter, inorganic compounds and radionuclides; many of which are currently used in U.S. water quality monitoring (Meybeck and Helmer, 1989; United States Environmental Protection Agency [USEPA], 2002a). These descriptors have allowed monitoring programs to identify, characterize and even attempt to remediate those water bodies considered polluted.

In an attempt to deal with surface water degradation, the United States Congress passed the Clean Water Act in 1972, requiring by law that states must identify and restore all polluted waters within their borders to acceptable water quality levels (33 USC 1313). The Clean Water Act has been largely successful at controlling and/or eliminating pollution threats from point sources, such as wastewater treatment plants and industrial discharges, but has been found to be deficient in its ability to manage non-point source pollution, such as runoff from urban and agricultural lands (Cooter, 2004; United States Geological Survey [USGS], 1996). These sources are more difficult to monitor and adequate characterization of a water body often requires significant time and resources to properly sample and process water quality data, making it impractical to monitor every stream, river and lake (Cooter, 2004).

The Passive Surface Water Flux Meter (PSFM) is described here as a new method for surface water quality analysis. The PSFM is a sister device of the Passive Flux Meter (PFM), which is currently being used for groundwater water quality monitoring (Hatfield et al., 2004; Annable et al., 2005; Clark et al., 2005). Both devices measure time-averaged solute and water fluxes at discrete locations without the aid of electronic hardware or external controls, but the PSFM does so in surface waters instead of groundwater (Hatfield et al., 2002). The low cost and passive nature of the device makes it practical for large-scale field applications, such as developing Total Maximum Daily Loads (TMDLs), by requiring little expense or manpower to use and maintain the PSFM device. The cumulative measurements ensure sampling has taken place throughout the length of the deployment and directly integrates measurements of discharge and solute

concentration to yield total flux, thereby reducing the number of separate measurements that must be made.

1.1.1 Total Maximum Daily Loads (TMDLs)

According to the Clean Water Act of 1972, each state, territory or tribe is required to develop a list of impaired waters and establish ambient water quality standards for each lake, river and stream based on their designated use(s). For all water bodies that do not meet these standards, a TMDL must be developed and implemented.

The TMDL was established under the Act as a means for quantifying the maximum amount of a pollutant that a water body can receive and still meet water quality standards (33 USC 1313). A TMDL must be created for each pollutant and should represent the sum of allowable loads for the contaminant including background levels, point and non-point sources, and a margin of safety to account for uncertainties (33 USC 1313).

Total maximum daily load development takes years and relies on one or more load assessment approaches to determine water quality standards for a particular water body. Assessments are made on a geographical (i.e., watershed) basis and must recognize and respond to a multitude of pollutants coming from not only surface waters, but groundwater and atmospheric deposition (USEPA, 1991). The level of effort needed to create a TMDL depends on the size of the geographical basis, the severity of impairment, and contaminants present (USEPA, 1991). Logically, inclusive large-scale watershed assessments require significantly more resources than small watershed or stream assessments, but can not be disregarded because they are necessary for investigating regional and national water quality.

Due to the intensive, long-term nature of the TMDL process, states often solicit other agencies and firms to monitor water quality. Frequently, the United States

Geological Survey (USGS) is called upon because its involvement in national programs such as the National Water-Quality Assessment (NAWQA), the National Stream Quality Accounting Network (NAS-QAN), the National Water Information System (NWIS) and a nationwide stream-flow gaging network; all programs that have been monitoring stream data since the early 1900's (USGS, 2000). The information from these USGS programs provides valuable background data useful for establishing water quality criteria, and help state agencies develop monitoring plans that will optimize sampling frequency and location, and aid in data analysis and interpretation (USGS, 2000).

1.1.2 Current Methods for Determining Contaminant Loads

Water quality indicators are typically measured in terms of contaminant concentration C_m [M/L^3], or contaminant load M_Q [M/T], which is defined as the maximum amount of contaminant a water body may receive in a given time period and still meet water quality criteria (USEPA, 2002a; Florida Department of Environmental Protection [FDEP], 2004a; FDEP, 2004b; FDEP, 2004c). Measurements of stream discharge Q [L^3/T] and contaminant concentration C_m [M/L^3] are often collected simultaneously as separate point discharge and point concentrations. Total loads are determined from these point values by integrating with respect to time

$$M_Q = \int \mathrm{Q} \cdot C_m dt \,. \tag{1-1}$$

Water flow, or discharge, is typically calculated from instantaneous measurements of stream stage and velocity across a channel transect over a given period of time. Stage measurements are usually taken directly using float devices or a variety of instruments that rely upon electrical, ultrasonic, or electromagnetic signals to detect and record changes in water levels (John and Haberman, 1980; Gupta, 1989). Stage data can then be

used to calculate the cross-sectional area for the channel's width at this transect. This area may then be combined with velocity data to determine Q as follows:

$$Q = \sum A_{ch} v \tag{1-2}$$

where A_{ch} [L^2] is the cross-sectional area of a channel transect and v [L/T] is the average velocity. The same information can also be obtained from *in-situ* hydraulic devices, such as weirs, orifices and flumes, all of which use specialized equations to quantify discharge directly (John and Haberman, 1980).

Stream water velocity is measured either automatically or manually, usually as a time-series of point measurements. Manual velocity measurements are typically taken with a hand-held flow meter, usually either current or acoustic doppler, and are recorded at several depths along each section of the channel profile to yield an average velocity for each section (Gupta, 1989; Webb et al., 1999; USEPA, 2001). The most commonly used methods are the two-point and six-tenths-depth methods, where velocity readings are taken as the mean of 0.2 and 0.8 depths or at 0.6 depth, respectively. In cases where channel walls are irregularly shaped, average velocity can not be expected to be at 0.6 depth. Therefore, anywhere between 3-10 velocity point measurements are taken at several depths along the vertical profile.

The stream water contaminant concentrations can be measured by manual collection, with autosamplers, or with *in-situ* probes designed to detect specific analytes (USEPA, 2001; Wang et al., 2004). Special precautions must be taken when collecting water samples to ensure that the sample is protected from degradation or outside contamination (USEPA, 2001). The depth and location at which the sample is collected must be taken into account. Just as flow velocity varies within a channel, concentrations

also may not be uniform. Therefore, methods similar to those used for water velocity measurements are also used when collecting water samples to ensure that representative average concentrations are taken (Webb et al., 1999; USEPA, 2001). Individual samples are then combined with discharge data to calculate total loads using Eq. (1-1).

As with water flow measurements, solute samples must be collected on an appropriate time-scale to accurately characterize the system being studied (Webb et al., 1999; USEPA, 2001). This is particularly important when looking at non-point source contamination. Heavy rainfall and poor drainage can move large quantities of contaminants through a given system in a short period of time. Sampling schedules often do not coincide with these storm events, and even autosamplers can be overloaded during events that last for an extended period of time.

1.2 Study Rationale

When taking into account the error associated with current methods for measuring water flow and the uncertainty associated with infrequent sampling; a method for measuring continuous water and solute fluxes seems appropriate.

The PSFM is a low-cost, low-maintenance device that directly measures average water flux (velocity) and average solute flux. Flux could be considered a more useful method for quantifying contaminant transport in streams because neither water flux (v) nor solute flux (J), requires knowledge of the cross-sectional area of the channel, a variable often difficult to calculate with accuracy. Therefore, measuring contaminants in terms of solute flux, or mass of contaminant per unit area-time, eliminates a source of inaccuracy incurred by estimation of A_{ch} in relatively steady flow systems.

Because the PSFM could produce a more accurate estimation of pollutants in stream channels, it may be useful for the restoration of impaired water bodies. Almost

half of the waters reported to the EPA as impaired cited agriculture as the source of pollution and one-fifth cited nutrients as their main pollutant (USEPA, 2002b). Most of these nutrient-impaired waters list nitrogen (N) and phosphorus (P) as the main sources of pollution.

Currently, eutrophication problems occur throughout the United States and have recently become a major concern. Most eutrophication problems arise when an excess input of N and/or P accumulates in a surface water body and starts to such a level that aquatic ecosystems and water quality are affected. Many problems have been linked to eutrophication including decreased dissolved oxygen contents, algal blooms and a general decrease in biodiversity, many of which can affect a water body's usefulness for human consumption and recreation (Carpenter et al., 1998; USEPA, 1999). Most nutrient inputs occur via non-point source runoff from urban and agricultural activities, making it difficult to quantify and regulate (Carpenter et al., 1998). In particular, Parry (1998) reported that nutrient pollution from agricultural sources accounts for more than 60% of impaired rivers and 50% of impaired lakes in the USA.

A great deal of water quality management in Florida is focused on problems associated with eutrophication due to P enrichment. Excessive fertilizer application, the destruction of small natural wetlands and the creation of drainage ditches have all contributed to P problem on a local and state-wide scale (Krazner, 2005). In particular, the Everglades National Park, a naturally oligotrophic wetland system, has been adversely affected by increased P inputs from a combination of urban and agricultural development (Perry, 2004).

The extent to which eutrophication occurs depends not only on the nutrient load, but on the flow of the river or stream (USEPA, 1999). It is known that advective transport is the primary transport mechanism of solutes in surface waters, and that flow rates and water depths can have a considerable effect on their distribution (Reddy et al., 1999). The flow regime within a channel most obviously affects water depth and velocity, but also indirectly affects temperature and the residence time of nutrients and gases. In general, higher flow rates are typically negatively correlated to P removal and sequestration by sediments and vegetation (Reddy et al., 1999). Slower flows allow nutrients to remain in one reach of a channel for a longer time period, increasing the availability to plants and bacteria by prolonging the residence time. Flow also affects the amount of turbulence and re-aeration that occurs within a channel, which indirectly may alter nutrient uptake by plants (USEPA, 1999). In systems where phosphorus is a likely pollutant, water quality monitoring may also be useful for determining the source of the P and the expected maximum concentrations. Therefore, the low-maintenance PSFM could be a useful tool for monitoring P transport in flowing surface water bodies since its design would allow solute fluxes to be calculated along the stream velocity profile at any number of locations over extended time periods.

In this study, phosphate (PO_4^{3-}), was chosen as the contaminant of interest because of its frequent listing as a major pollutant impairing streams throughout the United States. However, before the PSFM is applied to the field, the ability of this new device to accurately measure v and J under steady-state and transient conditions must be tested. The validation of the conceptual model of the PSFM under these flow conditions will be

the first step towards using this low-cost, low-maintenance PSFM design as a revolutionary new tool for surface water quality and TMDL monitoring.

1.3 Objectives

The objectives of this study were to 1) design and build a physical prototype PSFM 2) experimentally validate the conceptual and mathematical PSFM model outlined in Klammler et al. (2004), 3) test the hydraulic properties and functional velocity ranges for two PSFMs with different shapes, and 4) characterize and verify the ability of the PSFM to accurately measure point solute and water flux under steady-state and transient conditions.

CHAPTER 2
THEORETICAL BACKGROUND AND DEVICE DESIGN

2.1 Introduction

The conceptual model of the Passive Surface Water Flux Meter (PSFM) describes a self-contained, passive unit capable of directly measuring water and solute fluxes at a discrete location within a flowing surface water channel (Hatfield et al., 2002; Klammler et al., 2004). The PSFM model consists of a permeable, sorptive cartridge that is connected to openings in the surface of an impermeable, symmetric, streamlined body (Figure 2-1). When submerged in a flowing system, the profile of the PSFM creates a pressure gradient along the perimeter of the device inducing flow through the cartridge. Each cartridge is packed with a sorptive porous media impregnated with a known mass of a resident tracer. This tracer elutes from the cartridge at a rate proportional to the stream flow, while at the same time sorbing and retaining solutes dissolved in the water. After retrieval, the media is analyzed in the laboratory to determine the mass of solutes sorbed and mass of tracer remaining, giving estimations of water and solute flux, respectively.

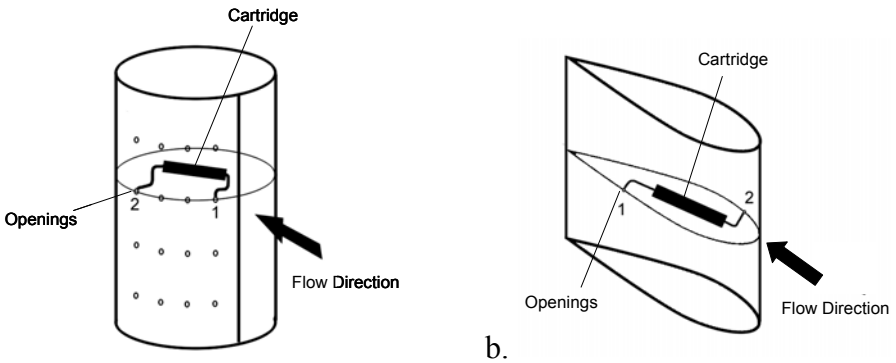

Figure 2-1 Schematics of PSFMs of different shapes: a) cylindrical, and b) hydrofoil. Water enters via opening 1 and exits through opening 2.

Flow through the cartridge a function of the pressure gradient along the surface of the device. It is well known that the velocity distribution on the surface of an impermeable cylinder may be calculated if for a given flow field (Green, 1939). To find the velocity distribution along a hydrofoil shaped device, conformal mapping must be used to relate the velocity distribution of around the cylinder to that found around a differently shaped object. Upon knowing this distribution, the pressure gradient along the profile of the PSFM may be determined. A significant, stable pressure distribution around the PSFM is necessary for measuring water and solute fluxes; therefore, several initial conditions must be met. Different flow conditions may affect the boundary layers, and therefore the pressure distribution, along the surface of an object submerged in a flow field (Zdravkovich, 1997). To maintain a stable pressure gradient, wakes should be prevented from forming behind the device to decrease the possibility of interference at the boundary layer where the openings are located, a phenomenon that might interfere with the flow field and thus with the calculation of water and solute fluxes (Klammler et al., 2004).

A steady pressure distribution also depends on the ratio of the channel's dimensions to those of the PSFM. As detailed in Klammler et al. (2004), three-dimensional flow around the PSFM should be avoided to minimize the occurrence of flow disturbances. To meet these conditions, the PSFM should be inserted vertically into the stream flow and be large enough to extend the entire depth of the channel. The width of the device should be small enough that edge effects from the channel walls do not interfere with the flow field around the PSFM. In this study, a channel-to-PSFM ratio of 2.5:1 was estimated as acceptable, where the maximum diameter of the PSFM was five times

smaller than the width of the channel, allowing 2.5 times the diameter of the PSFM on either side of the device.

2.1.1 Flow Field Determination

The conceptual model laid forth in Klammler et al. (2004) provides equations for determining the pressure difference as well as the local velocity at two openings on the PSFM. The pressure and velocity distributions around the submerged body can then be used to estimate the velocity of the flow field around it.

Since the shape of the PSFM defines the flow field around it, conformal mapping may be used to relate the complex potential of the flow field to the complex coordinates of the device. The flow field around a cylinder was adapted to that of a Joukowsky (hydrofoil) profile by Klammler et al. (2004) as follows:

$$z_j = \left[z_c - (1-b)\cdot a\right] + \frac{(a\cdot b)^2}{\left[z_c - (1-b)\cdot a\right]} \tag{2-1}$$

where $z_c = x_c + iy_c$ represents the complex coordinates of an impermeable circle with a radius of a [L], $z_j = x_j + iy_j$ are the transformed complex coordinates of the Joukowsky profile in the z_j-plane, b is a dimensionless parameter defining the shape of the profile by the chord-to-width ration, which ranges between 0 to 1, where $b = 0$ defines a circular (blunt) profile and $b = 1$ defines a profile that is a straight line (slender).

Using these transformed coordinates, Klammler et al. (2004) used v_j [L/T], the complex conjugate of the flow velocity around the PSFM to find v_o [L/T], the velocity of the flow field

$$v_j = v_o \cdot \frac{\left|1 - \frac{a^2}{z_c^2}\right|}{\left|1 - \frac{(a \cdot b)^2}{[z_c - (1 - b \cdot a)]^2}\right|} = v_o \cdot \chi_j \tag{2-2}$$

where χ [-], is a defined a proportionality constant that depends on the shape of the PSFM body and the locations of the two openings, points 1 and 2. Once the velocity at these points is known, the static pressures at these points can be determined using Bernoulli's equation

$$\left[\frac{p_1}{\rho g} + \frac{v_1^2}{2g} = \frac{p_2}{\rho g} + \frac{v_2^2}{2g}\right] = \left[\frac{1}{\rho g} \cdot (p_1 - p_2) = \frac{1}{2g} \cdot (v_1^2 - v_2^2)\right] \tag{2-3}$$

where p [M/LT^2] is the static pressure, v_1 and v_2 [L/T] are local velocities on the PSFM surface at openings 1 and 2, respectively, ρ [M/L^3] is the density of water, and g [L/T^2] is gravitational acceleration (Klammler et al., 2004). Eqs. (2-2) and (2-3) are then combined to yield water flux (velocity) v_o [L/T]

$$v_o = \sqrt{\frac{2g}{\chi_2^2 - \chi_1^2} \cdot \left(\frac{p_1}{\rho g} - \frac{p_2}{\rho g}\right)} \tag{2-4}$$

where v_o is determined by the static pressure differences an location of points 1 and 2.

Based on this, a known head difference between any two points may be used to calculate the stream velocity around the device if χ is known. Using the equations above, and known χ values, the velocity may be estimated for different head differences depending on the shape and location of the openings, as shown in Figure 2-2. This figure displays estimated velocities for a range of head differences based on real χ values used for the PSFM devices tested in this study.

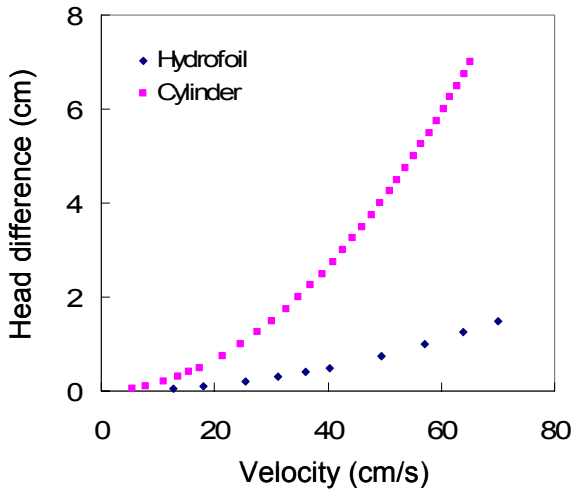

Figure 2-2: Estimated head-velocity relationships for two different PSFM devices. Larger head differences are produced at a given velocity using the known χ values for a cylindrical PSFM.

2.1.2 Flux Determination Under Steady State Conditions

Under steady state conditions, it is assumed that v_j, v_o, and the solute concentration in the water are constant throughout the time of the measurement. When these parameters are held constant, water flow through the cartridge, Q_c [L^3/T], can be measured by calculating the relative amount of resident tracer remaining on the cartridge. If the assumptions of linear, instantaneous, reversible sorption of the tracer are met, then Q_c may be calculated as follows

$$Q_c = -\frac{(M_{t,r} - 1)A\Theta R_t L}{t} \tag{2-5}$$

where $M_{t,r}$ [-] is the relative mass of the tracer remaining after elution time t [T] (determined by quantitative analysis of the cartridge) with respect to the initial mass of the tracer, A [L^2] is the cross-sectional area of the cartridge, Θ [-] is the porosity of the media, R_t is the retardation factor of the tracer and L [L] is the length of the cartridge (Klammler et al., 2004).

Hatfield et al. (2004) developed an alternate method where by non-linear tracer elution functions may be used to calculate water flow, by super-imposing a linear function over segments of the non-linear elution function. In this way, the elution may be described by different linear equations for different ranges of relative mass remaining (Figure 2-3). Using this technique, a new R_t may be calculated for each linear segment of the elution curve

$$R_t = \frac{1}{\sum_{i=1}^{p} \frac{\varphi_i - \varphi_{i+1}}{R_{di}}}. \qquad (2\text{-}6)$$

Here, i (i=1, 2,…, p) denotes each segment of the linear approximation, $\varphi_i - \varphi_{i+1}$ represents the mass fraction eluted according to the linear segment and R_{di} is the retardation factor for i (i=1, 2,…, p). These parameters are all determined directly from the plot of the linearized pieces, where R_{di} is obtained from the terminating abscissa of segment i and φ_i is the intercept of segment i on the y-axis (Hatfield et al., 2004). The R_t values calculated in Eq. (2-6) may then used in Eq. (2-5) for the appropriate $M_{t,r}$.

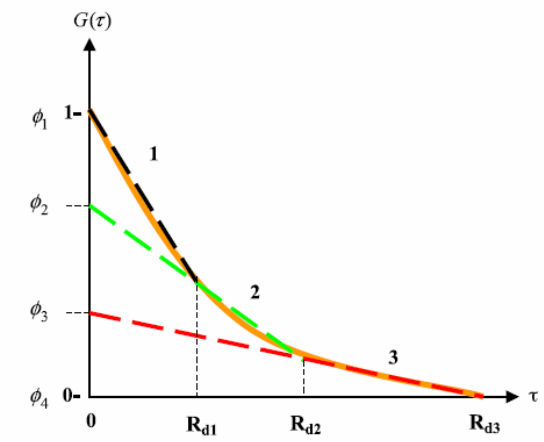

Figure 2-3: Linearized segments fit to a general non-linear elution curve. Here, three linear segments have been fit to the non-linear elution function $G(\tau)$ where φ_i and R_{di} define each segment [Reprinted from Hatfield et al. 2004].

After Q_c has been evaluated, the head difference across the cartridge is estimated using

$$\Delta H = \left(\frac{p_1}{\rho g} \cdot \frac{p_2}{\rho g} \right) = (1 - M_{t,r}) \cdot \frac{L^2 \Theta R_t}{Kt} \tag{2-7}$$

where K [L/T] is the hydraulic conductivity of the porous media within the cartridge. Equation (2-7) may then be used to calculate v_o from Eq. (2-4) if the χ values of the openings are known.

While Q_c and ΔH can be described by a linear relationship, Figure 2-2 shows that the relationship between head difference and velocity is not linear. Therefore the relationship between stream velocity and the flow rate through the PSFM cartridge will not be directly proportional.

Solute mass flux J_s [M/(L^{2}T)] may be calculated with the equation

$$J_s = v_o \cdot C_s \tag{2-8}$$

where flux measurements rely on estimates of the stream velocity, found using Eqs. (2-7) and (2-4), and on the mass yield of the solute of interest from the sorptive media within the cartridge (Klammler et al., 2004). The total mass of the solute M_s [M] retained by the sorptive media is determined by quantitative analysis and used to estimate the concentration of the solute C_s [M/L^3] in the stream flow where

$$C_s = \frac{M_s}{Q_c \cdot t} \ . \tag{2-9}$$

It is important to note that C_s will be calculated incorrectly if any solute exits the cartridge. Therefore, it is important to replace the cartridges before the sorption capacity is exceeded. The duration of deployment is estimated based on the retardation factor associated with a particular solute and the expected flow rate though the column. High

flow rates may introduce non-equilibrium conditions, limiting sorption and therefore affecting the final calculation of C_s.

2.1.3 Flux Determination Under Transient Conditions

Transient conditions more closely represent natural systems and therefore are important to take into consideration. Under steady-state conditions, the area of the stream channel is assumed to be constant. Natural channels often are irregularly shaped, causing stream flows to change in cross-sectional area depending on their stage height. Variations in both v_o and A_{ch} are problematic when trying to estimate water velocity with a PSFM under transient conditions.

In general, the water velocity v_o can be described by

$$v_o = \sum \frac{Q(t)}{A_{ch}(t)} \tag{2-10}$$

where it can be seen that if $A_{ch}(t)$ is constant, v_o is directly proportional to Q. In cases where $A_{ch}(t)$ varies with time, there is no direct way to calculate Q without the aid of additional equipment. Therefore, in this study transient studies were conducted only by varying solute flux while maintaining a constant water velocity.

When flow remains relatively steady, the water and solute fluxes can be calculated using the equations developed for steady state conditions, only the solute flux will now represent an average solute concentration in the stream channel over the duration of deployment. This average concentration is a direct result of the measurement itself being time-averaged, therefore no estimates on the concentration range over that time period may be made.

2.2 Development of a Passive Surface Water Flux Meter

Physical prototypes were developed to verify the conceptual model as described in Klammler et al. (2004) and to test the ability and accuracy of these devices for measuring water and solute fluxes. The PSFM was developed in two parts; the impermeable body and the permeable, sorptive cartridge.

2.2.1 PSFM Body Development

Since a wide range of flow conditions may be experienced in the field, this study examined the plausibility of using differently shaped devices for different flow regimes. In theory, PSFM shapes can be selected to best fit the expected flow regime. Blunt shapes create larger pressure gradients than more slender shapes at slower velocities (as shown in Figure 2-2), but also develops wake formations before their more slender counterparts. Prototype bodies with two different shapes [b = 0.85 (hydrofoil) and b = 1.0 (cylinder)] were constructed to compare their ability to measure water and solute fluxes under various channel velocities.

This study tested four devices: a cylindrical PSFM and three successive generations of hydrofoil PSFMs. All four were constructed with a rigid outer body and openings along a portion of the device. The openings were installed at several different heights along the vertical profile of each device with several openings per "level" so that fluxes could be measured at various heights and pressure gradients.

The first two generations of hydrofoil PSFMs were constructed in a similar manner; both devices consisted of a vertical rod (spine) mounted on a horizontal base with several wooden "ribs" positioned along the length of the spine. The wooden ribs were cut to a chord/width ratio where b=0.85, and were spaced evenly along the spine. The first hydrofoil (HF1) was made of fiberglass with h = 35 cm and L = 19.5 cm (Figure

2-4a). The second generation (HF2) with h= 26.3 cm and L= 19.5 cm was fabricated by molding plastic around wooden ribs identical to those used in the first generation (Figure 2-4b). The third generation hydrofoil (HF3) has an h=64.1 cm and L=51 cm and was formed by molding plastic to into a shape of b=0.85, eliminating the wooden frame and ensuring a better profile form (Figure 2-4c). The cylinder PSFM (h=40 cm, D= 11.4 cm) was made from a section of PVC pipe. Four openings were drilled into one front quadrant of the device at four different heights. The device was mounted vertically to a rod for stability during experiments (Figure 2-4d).


a


b

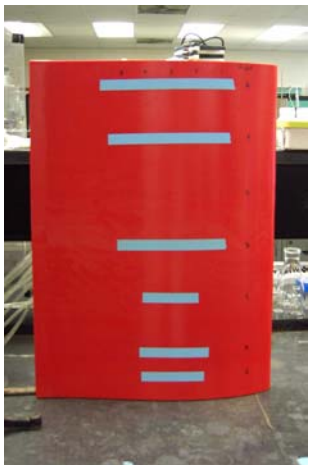
c

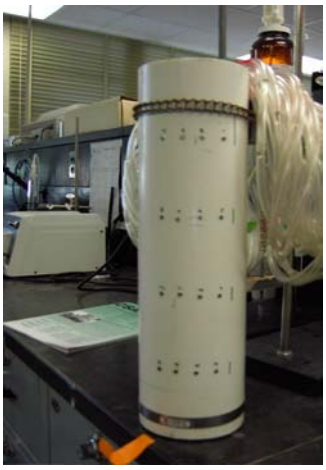
d

Figure 2-4: Four PSFM devices used to calculate water and solute fluxes. a) first prototype of the hydrofoil-shaped PSFM (HF1) b) second hydrofoil-shaped PSFM (HF2) c) third prototype of the hydrofoil-shaped PSFM (HF3) d) cylindrical-shaped PSFM.

2.2.2 PSFM Cartridge Development

Three different methods were evaluated for estimating water and solute flux. The first investigated the use of a visual dye tracer as the resident tracer. The other two approaches each used a form of non-visual, organic resident tracer. Each method was tested using a different type of cartridge. The type of porous media associated with each method/cartridge varied depending on the resident tracer used.

All cartridges were made using Kontes borosilicate glass columns with 500 μm polypropylene mesh filters (Spectrum Labs, Inc.) and a Kontes nylon three-way valve at each end. The cartridges were connected to the body of the PSFM by Tygon tubing. The direction of flow through the column was controlled by connecting the inlet of the column to the port with the highest static pressure.

To pack the cartridge, a slurry of the porous media was made by submerging the solids in their original supernatant, or in deionized (DI) water when no supernatant was available (i.e. ion exchange resins). The slurry was poured into the bottom of the cartridge and vibrations were applied to tightly pack the material and release any trapped air bubbles. Once full, and the cartridge was sealed using the three-way valves to close the cartridge either end until ready for use.

The first method used cartridges (L= 15 cm, I.D. = 2.5 cm) that were packed with Dowex Marathon MSA anion exchange resin. This media acted both as a sorbent for the solute of interest, phosphate, and as a non-reactive matrix through which a dye tracer could travel. Dye was injected via a three way valve on the influent end of the cartridge, and displacement through the column was tracked visually. Upon completion of the

experiment, the cartridge was dissected, sectioned, and analyzed for phosphate. No chemical analysis of the dye tracer was necessary.

The second method used cartridges (L= 10 cm, I.D. = 1.5 cm) that were packed with Lewatit S6328A anion exchange resin and an organic resident tracer made of 246 ppm 1-heptanol, 2-octanol, and 165 ppm 2-ethyl-1-hexanol and 1-octanol. Water and solute flux measurements were made by analyzing the column contents. The resin was removed and well-mixed to ensure homogeneity before being divided for analysis.

The third approach used cartridges (L= 10 cm, I.D. = 1.5 cm), packed with two different kinds of porous media. The Lewatit S6328A anion exchange resin was packed into the first 45% of the cartridge for the sole purpose of sorbing phosphate. The remainder of the column was filled with activated carbon pre-equilibrated with a suite of organic tracers: 1000 ppm each of methanol, ethanol, isopropyl alcohol (IPA), and *tert*-butyl alcohol (TBA), and 500 ppm 2,4-dimethyl-3-pentanol (2,4 DMP). Analysis of water and solute fluxes was performed by removing the resin from the activated carbon, then analyzing the resin for M_s, the amount of PO_4^{3-} sorbed, and the activated carbon for $M_{t,r}$, the amount of tracer remaining.

2.3 PSFM Hydraulic Analysis

The conceptual model of the PSFM was first tested by verifying the existence and range of the predicted pressure gradient along the surface of the device. Ancillary experiments were performed to investigate the accuracy with which the PSFM could estimate stream flow velocities.

2.3.1 Laboratory Experiments

Cartridges were first calibrated under known conditions before use in experimental trials. Calibrations were done to find the hydraulic conductivity of the cartridge's porous

media by estimating the relationship between specific discharge and hydraulic gradient. These studies were also used to estimate the proper duration of deployment.

Cartridges were fit on either end with manometers so that pressure differences across the column could be accurately measured. The cartridge was attached to a constant head reservoir consisting of a 10 L Marriott bottle filled with PO_4^{3-}-spiked DI water. The height of the reservoir was adjusted to create known pressure gradients and the water discharged from the column was collected and measured (Figure 2-5). Darcy's Law was used to relate the specific discharge q [L/T] and the hydraulic gradient dH/dl [-]

$$q = \frac{Q}{A} = -K\frac{dH}{dl} \tag{2-11}$$

where A [L^2] is the cross-sectional area of the column and K [L/T] is the hydraulic conductivity of the porous media.

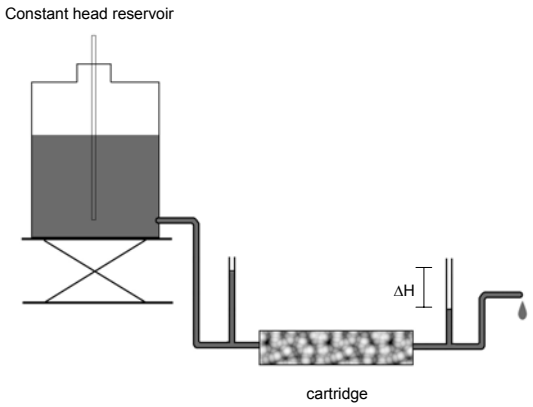

Figure 2-5: Diagram of cartridge calibration apparatus. Changes in the elevation of the constant head reservoir are directly proportional to the change in dH/dl.

2.3.2 Laboratory Results

Results from the visual tracer method showed the resin had a K = 9.8 cm/min. The resin used in the second method had a K= 16.7 cm/min and the resin/activated

charcoal combination used in the third method had a combined *K*= 18.3 cm/min (Figure 2-6a-c).

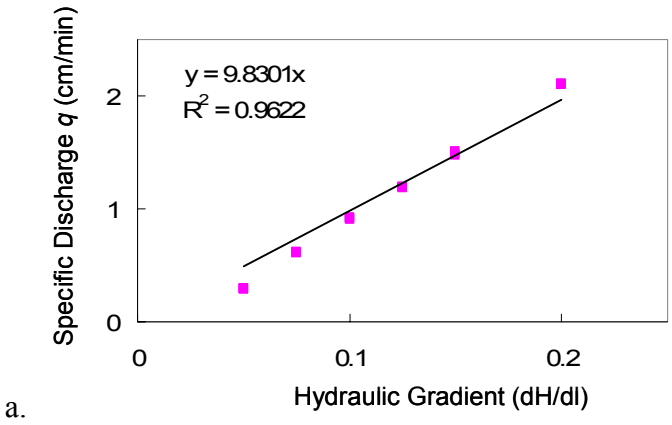

a.

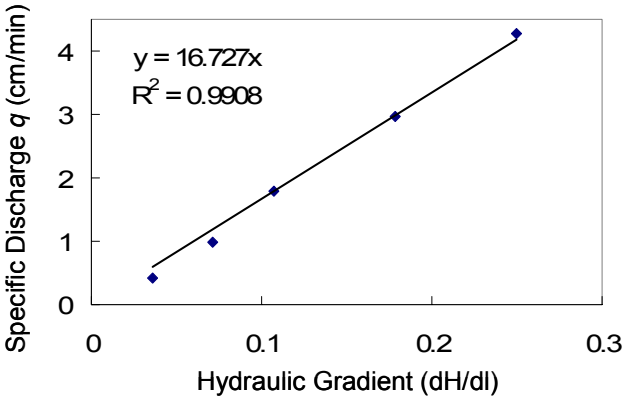

b.

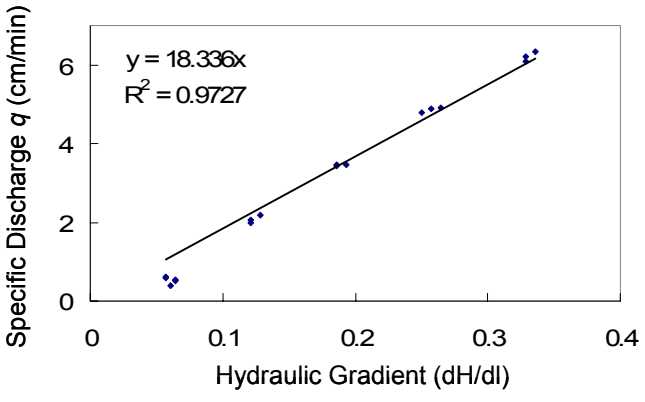

c.

Figure 2-6: Calibrations for three different types of porous media. a) visual tracer method b) organic tracer (resin-only) method c) organic tracer (resin and activated carbon) method.

2.3.3 Flume Experiments

Flume experiments were performed in a rectangular (L = 18 m, w = 0.6 m), recirculating flume at the Coastal Engineering Laboratory at the University of Florida. Flume velocities were controlled using a crank ball valve and further adjusted with the use of an underflow weir located at the end of the flume channel. Local tap water from Gainesville Regional Utilities was used in all flume experiments.

The velocity of the water in the flume v_o [L/T] was estimated using the equation

$$v_o = \frac{Q_{ch}}{w_{ch} \cdot h_w} \tag{2-12}$$

where w_{ch} is the width of the flume channel and h_w is the height of the water. The flume discharge Q_{ch} was obtained from the underflow weir equations developed by Prathaba et al. (1992)

$$Q = C_d \cdot ab(2gh_o)^{1/2} \tag{2-13}$$

$$C_d = 0.611 \cdot \left(\frac{h_o - a}{h_o + 15a} \right)^{0.072} \tag{2-14}$$

where C_d [-] is the discharge coefficient, a is the gate opening [L], b is the channel width [L], g is gravitational acceleration [L/T^2] and h_o is the approach flow depth [L]. Water velocity profiles in the flume were also measured in some experiments using an acoustic doppler velocimeter, or ADV (SonTek FlowTracker Handheld ADV). The PSFM devices were deployed in the center of the channel a sufficient distance from the underflow weir to avoid any perturbations in velocity due to the gate opening. U-tube manometers were made from the device tubing before being attached to the cartridges so that static pressure differences could be measured. The cartridges were then attached to

the body of the PSFM with the influent end connected to the opening with the higher static pressure and the effluent end to the opening with the lower static pressure.

2.3.4 Flume Results

The true water velocity within the flume was calculated using both an underflow weir equation v_{weir} (Eq. 2-13) and the acoustic doppler velocimeter v_{ADV}. Comparison of these two measurement techniques revealed a 12% difference between the two measurements (Figure 2-7). The strong correlation (R^2=0.94) between the two techniques suggested either technique could be used to measure true water velocity; therefore, all experiments compared estimated water fluxes to those measured by the ADV. The ADV was selected to represent true water flux since velocity profile information could be obtained with this device. This is particularly advantageous since local estimated vs. measured velocities may be compared along each sampling level of the PSFM.

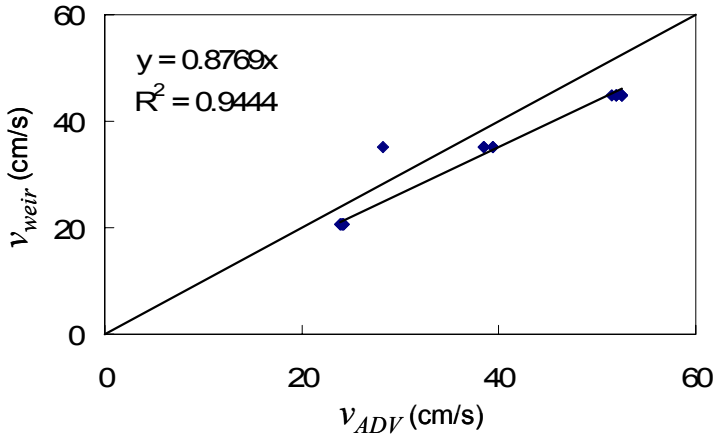

Figure 2-7: Comparison of "true" water velocities using a resin/tracer PSFM. A one-to-one line shows the 12% difference in measurements made by the underflow weir vs. the ADV.

Stream flow velocity v_H [L/T] was calculated by measuring the difference between the static pressures at two points on the PSFM body. The known ΔH

and χ values were applied to Eq. (2-4) and compared to true velocities calculated using the underflow weir Eq. (2-13) and those estimates made using an ADV (Figure 2-8).

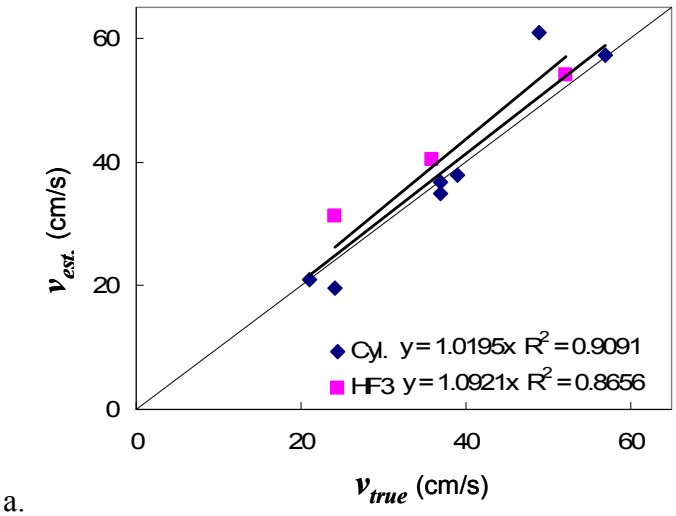

a.

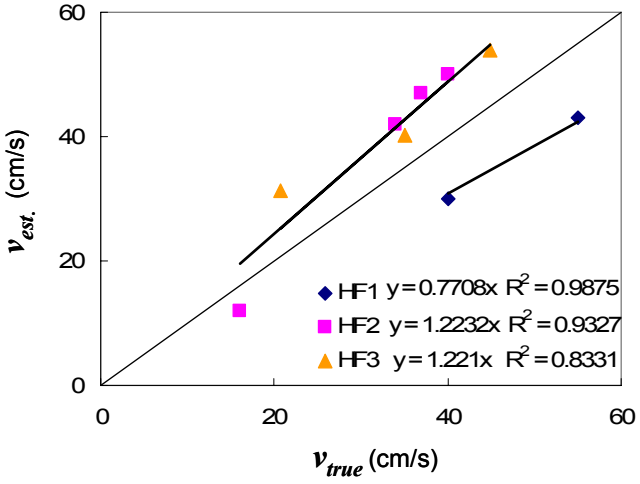

b.

Figure 2-8: Comparison of estimated vs. true stream velocities based on differences in head. a) true velocity v_{true} is measured by ADV, estimated velocities are measured using the cylindrical and 3rd generation hydrofoil PSFMs b) true velocity v_{true} is measured with the underflow weir and compared to velocities estimated using three generations of hydrofoil PSFMs.

Results showed estimated velocities were within 2-10% of the true stream velocity when compared against the ADV measurements (Figure 2-8a). The cylindrical PSFM performed slightly better than the hydrofoil shaped device (HF3), but a lack of conclusive data about the hydrofoil PSFM leaves the accuracy of this device unknown. Data from

Figure 2-8b shows estimates made using the hydrofoil PSFMs and the sluice-gate equation yield a higher percent difference, but when true stream velocities are adjusted by 12%, or the difference between the ADV and sluice-gate velocity measurements, the ability of the hydrofoil PSFMs to estimate true water velocity are on par with those made using the ADV measurements. The only exception is the first generation hydrofoil PSFM (HF1) who under-predicts the true velocity by ~33%. The first prototype's information may be neglected since all studies were performed with successive generations. Therefore, it may be concluded that either device may be used when estimating velocities in the range of 15-60 cm/s, the maximum range of the flume.

CHAPTER 3
WATER FLUX EXPERIMENTS

3.1 Introduction

Accurate water flux estimations are important for determining mass loads in flowing surface water systems. Therefore, three combinations of porous media and resident tracers were tested; a visual dye resident tracer on ion exchange resin, a suite of organic alcohol tracers on ion exchange resin, and a suite of different organic alcohol tracers on activated carbon. Water velocities were measured using three techniques:

1. Head Difference (v_H)- denoted throughout the remainder of the manuscript as the subscript "$_H$," where the difference in static pressures at the ports was measured before the cartridge attached. This difference (ΔH) was then used to predict water velocity v_H according to Eq. (2-4).

2. Dye Movement (v_D)- denoted throughout the remainder of the manuscript as the subscript "$_D$" where the velocity of the dye was used to estimate the average flow rate through the cartridge. The estimated flow rate yields a ΔH which may then be used to predict water velocity v_D according to Eq. (2-4).

3. Tracer Remaining (v_T)- denoted throughout the remainder of the manuscript as the subscript "$_T$," where the relative mass of tracer remaining in the cartridge is used to determine the average flow rate through the cartridge. The estimated flow rate yields a ΔH which may then be used to predict water velocity v_T according to Eq. (2-4).

3.2 Porous Media Selection

The two types of porous media considered for use in PSFM cartridges were ion exchange resins and activated carbon. Activated carbon was chosen because it has been shown as an effective matrix for the elution of tracers in groundwater flux meters (Hatfield et al., 2004; Annable et al., 2005). The ion exchange resin was chosen for its high permeability, its ability to function under a wide pH range, and its known ability to

selectively sorb hydrophobic and charged solutes (i.e. PO_4^{3-}). In addition, the light surface color of the resin held potential for easy visual identification of dye tracer.

One silver-impregnated granular activated carbon (989 12_30: Barnebey Sutcliffe Corp., Columbus OH) and eight different ion exchange resins were selected for testing based on their availability and known physical characteristics (Table 3-1).

Table 3-1. Ion exchange resins tested for PSFM use.

Resin Name	Type	Structure	Manufacturer	Manufacturer's Comments
Dowex Marathon MSA	anionic, strongly basic	macroporous	Dow	well suited for use in high organic waters and has very good fouling resistance
Lewatit S6328A	anionic, strongly basic	macroporous	Sybron Chemicals Inc.	use with hydrophilic high molecular weight anionic substances and colorants
Macro-T Bryon	anionic, strongly basic	macroporous	Ionac Brand	
Amberlite	anionic, strongly basic	gel	Rohm and Haas	high chemical resistance and excellent resistance to fouling
Dowex Marathon 11	anionic, strongly basic	gel	Dow	well suited for use in high organic waters and has very good fouling resistance
Supelite DAX-8	non-ionic	gel	Supelco, Inc.	good for environmental analysis, organics and wastewater treatment
Cabsorb	cationic, zeolite	crushed mineral	GSA Resources, Inc.	

3.3 Visual Tracers

Dye tracer studies are commonly used for tracing water flow paths both in the laboratory and in the field. Due to their frequent use, some dyes, such as Rhodamine

WT, Brilliant Blue, and Acid Yellow 73, have been well characterized in terms of their sorption properties and compatible media types (e.g., Smart and Laidlaw, 1977; Kasnavia et al., 1999; Stern et al., 2001; Kasteel et al., 2002). Few, if any, studies have been done using dyes as tracers on ion exchange resins. Resins and other sorbents (e.g., activated carbon, fly ash, tree bark, rice husks) have been thoroughly tested for their ability to remove dyes from wastewater (Faria et al., 2004; Karcher et al., 2001; Karcher et al., 2002; Morais et al., 1993; Sun and Yang, 2003), but little characterization has been recorded on dyes that were not strongly bound by sorbents. Therefore, dye/resin combinations were chosen based on general physical and chemical characteristics rather than cited literature.

3.3.1 Tracer Criterion

A visual tracer, such as a dye, was considered in this study as an alternative to a non-visual tracer when quantifying water flux. Dye tracers would be advantageous since the volume of water that had passed through the cartridge could be detected visually without sacrificing the entire cartridge.

In order for a dye tracer to be successful, it must 1) be chemically stable and readily detectable both in the laboratory and the field, 2) move along the porous media within the cartridge in plug-flow fashion, or in such a way that distance traveled by the dye could be easily related to the volume of water that has passed though the cartridge, 3) not interfere with the sorption or detection of the solutes of interest, and 4) be able to provide information during a range of time periods (i.e. hours, days, weeks) appropriate for field use. With these criteria met, water flux could then be determined by visual inspection of the cartridge, eliminating the need to analyze the tracer.

A transparent cartridge containing a suite of dyes, each with a different color and retardation factor, was proposed for the PSFM. The suite of dyes would contain several dyes expressing a range of retardation factors. One dye would represent the lifetime of the cartridge, serving as an indicator for when the cartridge should be replaced. Twelve dyes with a low toxicity and low cost (less than $2/g) were selected from Green (1991) based on their polarity and solubility in water (Table 3-2).

Table 3-2. Dyes tested for PSFM use.

Dye Name	CAS Number	Solubility	Ionic Charge
Basic Blue 3	33203-82-6	30 mg/mL	Cationic
Basic Yellow 11	4208-80-4	good	Cationic
Brilliant Green	633-03-4	40 mg/mL	Cationic
Chrysoidin	532-82-1	20 mg/mL	Cationic
Malachite Green	569-64-2	60 mg/mL	Cationic
Rhodamine 6G	989-38-8	20 mg/mL	Cationic
Amaranth	915-67-3	60 mg/mL	Anionic
Direct Red 23	3441-14-3	40 mg/mL	Anionic
Erioglaucine	3844-45-9	30 mg/mL	Anionic
Fluroescein	518-47-8	40 mg/mL	Anionic
Phloxine B	18472-87-2	90 mg/mL	Anionic
Rhodamine WT	37299-86-8	good	Anionic

3.3.2 Materials and Methods

Batch and column experiments were performed using different combinations of the 8 ion exchange resins and 12 dye tracers. Tracers were studied separately so that each dye could be characterized individually.

Batch experiments were performed to provide preliminary sorption information, and were analyzed by visual inspection only. Desired adsorption and desorption characteristics were based on the relative removal of dye from solution and the relative release of dye from the resin, respectively. Desorption studies were executed using tap water, since the chemical composition would be most similar to conditions found in field.

Column studies were used to measure dye movement in exchange resin. These experiments were performed by either packing a small layer of resin impregnated with the dye tracer near the inlet of a resin-filled cartridge, or by direct injection of dye into the cartridge. Tap water was allowed to flow through the column using constant head reservoirs for a minimum of 100 pore volumes. Dye movement along the length of the column was measured visually from the center of mass of the dye.

3.3.3 Results and Conclusions

A total of 4 dye/resin combinations were found to meet at least half of the criteria listed in Section 3.3.1 (Table 3-3). These combinations were:

- Basic Blue 3/Dowex Marathon MSA
- Basic Yellow 11/Dowex Marathon MSA
- Brilliant Green /Dowex Marathon MSA
- Malachite Green/Dowex Marathon MSA

Of the four possibilities, Basic Yellow 11 and Brilliant Green combinations were rejected because of continual desorption of dye into the supernatant, even after color appeared to have been removed from the resin. This was undesirable since PO_4^{3-} analysis was conducted using colorimetric techniques and any dye in the supernatant could affect results. The Malachite Green combination was rejected because of a possible Fenton-reaction chemical breakdown, explained by Dutta et al. (2003) as a known chemical reaction such that hydroxyl radicals in weakly acidic solutions degrade Malachite Green dye. This reaction was witnessed in laboratory experiments where loss of green color occurred within 48 hours.

Table 3-3: Tracer criteria met by dye/resin combinations. An "X" signifies that the criterion was met.

		Criteria Met			
Dye	Resin	1	2	3	4
Basic Blue 3	Dowex Marathon MSA	X	X	X	
Basic Yellow 11	Dowex Marathon MSA	X	X		
Brilliant Green	Dowex Marathon MSA	X	X		
Malachite Green	Dowex Marathon MSA		X	X	
Amaranth	Lewatit S6328A	X			
Amaranth	Macro T	X			
Amaranth	Dowex Marathon MSA	X			
Amaranth	Amberlite	X			
Amaranth	Cabsorb				
Amaranth	Dowex Marathon 11	X			
Basic Blue 3	Lewatit S6328A	X			
Chrysodin	Dowex Marathon MSA	X			
Direct Red 23	Dowex Marathon MSA	X			
Erioglaucine	Dowex Marathon MSA	X			
Erioglaucine	Amberlite	X			
Erioglaucine	Supelite	X			
Fluorescein	Amberlite				
Flourescein	Dowex Marathon MSA				
Malachite Green	Lewatit S6328A	X			
Phloxine B	Lewatit S6328A	X			
Phloxine B	Macro T	X			
Phloxine B	Dowex Marathon MSA	X			
Phloxine B	Amberlite	X			
Phloxine B	Cabsorb				
Phloxine B	Dowex Marathon 11	X			
Rhodamine 6G	Dowex Marathon MSA	X			
Rhodamine WT	Dowex Marathon MSA	X			

The combination that met the most criteria, Basic Blue 3/Lewatit, was used in flume experiments to visually determine stream velocity. Cartridges were first calibrated in the laboratory using Darcy's Law (Eq. 2-11) to measure the hydraulic conductivity, based on the ratio of the specific discharge q [L/T] and hydraulic gradient dH/dl [-] (Figure 3-1). This calibration was then used to compare the differences in q as determined by the volumetric measurement of effluent collected (q_D) and the velocity of the dye moving through the column (q_V) at different head gradients using the equations

$$q_D = \frac{V}{At} \tag{3-1}$$

$$q_V = \frac{L\eta}{t} \tag{3-2}$$

where V [L^3] is the volume of effluent collected, A is the cross-sectional area of the cartridge, t [T] is the sample collection time, L [L] is the distance the dye has traveled in time t and η [-] is the porosity of the media. As shown in Figure 3-1, the slopes of q_V and q_D are approximately equal, showing that dye is traveling at the same velocity as the water within the cartridge (R≈1). Based on these results, it was concluded that the dye provided accurate representation of the pore water velocity within the column, fully exiting the cartridge after one pore volume.

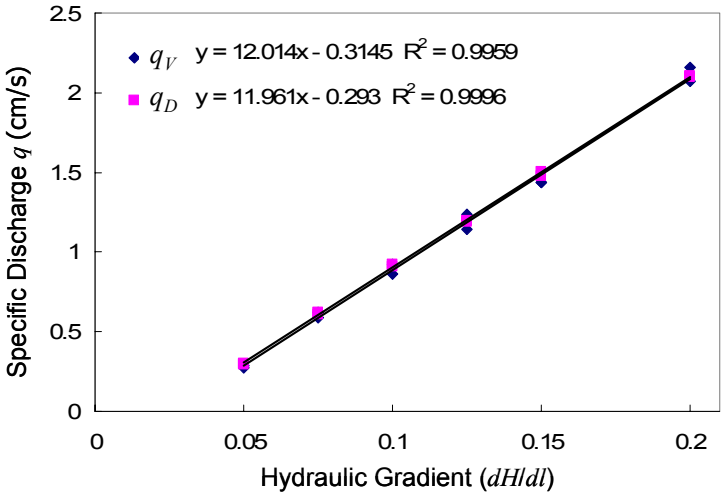

Figure 3-1: Comparison of specific discharge using two different methods. The slope of each line represents the measured hydraulic conductivity of the cartridge based on two different estimation techniques, q_V and q_D.

Based on these results, flume experiments were performed by using a three-way valve on the influent end of the cartridge to inject Basic Blue 3 into a glass column (I.D. = 2.5 cm, L= 24 cm) packed with Dowex Marathon MSA exchange resin. The dye travel time was used to estimate the velocity of water though the porous media. The head

gradient across the column was estimated based on the calibration relationship in Figure 3-1. These measurements were then used in Eq. (2-4) to solve for v_o (Table 3-4).

According to the flume experiments, the estimated water velocities differed from the true velocities by 0.8-12.5%. This difference was considered small and thus it was concluded that Eq. (2-4) was a valid equation for estimating stream velocities with a dye tracer over short time periods. Although this dye tracer showed promise in terms of it's ability to accurately water flux measurement, all dye/resin combinations tested had either an R≈1 or an R>>1, both of which were considered unacceptable for the time scale being studied here. Estimates made at higher velocities and/or over longer periods of time would ideally require a dye tracer with a retardation factor ranging from 3-500.

Table 3-4: Water flux measurements using a cylindrical PSFM and a dye tracer.

% Depth from Bottom	True velocity v_o (cm/s)	Estimated velocity v_D (cm/s)	Difference (%)
43	32.1	35.7	10.9
43	35.4	35.7	0.8
43	35.4	35.7	0.8
43	35.4	35.7	0.8
62	36.4	39.1	7.2
62	36.1	39.1	8.0
62	35.5	39.1	9.7
81	35.3	39.1	10.2
81	34.5	39.1	12.5
81	35.1	39.1	10.8

3.4 Organic Tracers

Previous works have shown that alcohols have been used successfully as resident tracers on activated carbon in groundwater studies using a passive flux meter (Hatfield et al., 2005; Annable et al., 2005). Since the PSFM is similar in nature to the groundwater passive flux meter, cartridges were tested using sorbents and resident tracers similar to

those described in Annable et al. (2005). In this study, an activated carbon matrix and ion exchange resin matrix were both evaluated for potential use with an organic resident tracer.

3.4.1 Tracer Criterion

The organic tracers selected for study were chosen using criteria similar to those listed for the dye tracers: 1) must be simple to remove and detect after deployment, 2) the mass lost after a given time period must be proportional to water flow through the column, 3) must not interfere with the sorption or recovery of the solutes of interest, and 4) must be able to provide information during a range of time periods appropriate for field use.

3.4.2 Materials and Methods

Two suites of organic tracers were examined, each with a different porous media matrix. Sorption/desorption properties of the two types of resin/tracer and activated carbon/tracer cartridges were characterized using column elution studies. The resin/tracer combination tested tracer elution properties at flow rates of 0.6 mL/min, while the activated carbon/tracer cartridges used flow rates of 3.1, 5.1 and 7.1 mL/min. Results from these experiments were used to predict tracer behavior during flume experiments.

Before deployment, the vertical velocity profile of the flume was characterized at each velocity using the ADV. In every case, the velocity profile was found to be nearly uniform, allowing cartridges attached to the PSFM at different water depths to serve as replicates (Figure 3-2).

Both types of cartridges were tested at similar velocity ranges in the flume, and velocities estimated using the static pressure difference (v_H) and the organic tracer (v_T) were compared to true water velocities (v_o) to determine how well the PSFM performed.

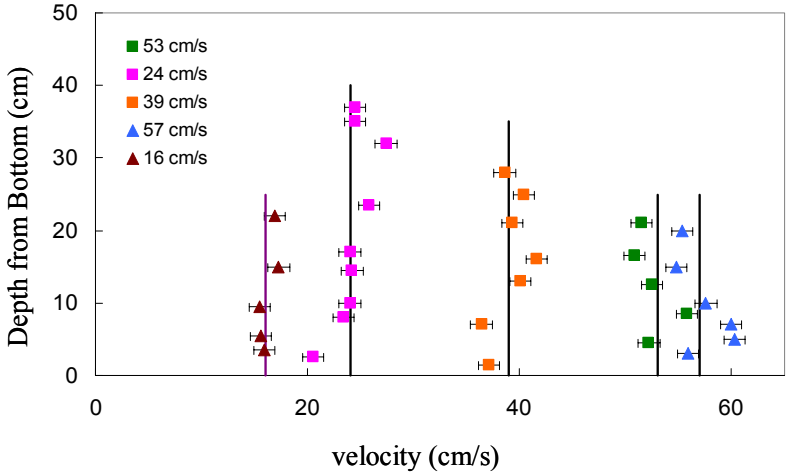

Figure 3-2: Velocity profiles for the range of velocities tested in the flume. The maximum range of the flume was ~15-60 cm/s.

Resin/tracers. The first combination tested used Lewatit S6328A as the sorbent and the following four alcohols as the suite of resident tracers: 1-octanol (165 ppm), 2-ethyl-1-hexanol (165 ppm), 2-octanol (246 ppm) and 1-heptanol (246 ppm). Before loading the resin with tracer, the Lewatit was first washed in isopropyl alcohol (IPA), the experimental extraction solvent, to remove impurities that were found to interfere with the tracer peak detection. The resin was then drained and rinsed with DI water. After rinsing, 1-L of the water-based tracer solution (listed above) was added to the resin and placed on a shaker table to equilibrate for ~24 hours. After equilibration, the resin was drained and packed into glass columns (L = 14cm, I.D. = 1.5 cm) using techniques described in Section 2.2.2.

After deployment, the cartridges were dissected, and the resin was homogenized by thorough stirring before equilibration with IPA for tracer extraction. Samples were

allowed to equilibrate for ~24 hours at a reciprocating speed of 25 rpm, then were removed and placed in a refrigerator to settle for ~12 hours. Tracer mass remaining was analyzed by GC/FID.

Activated carbon/tracers. The second method tested a pre-made combination of a suite of five alcohol tracers on activated carbon. The alcohol tracers sorbed to the activated carbon were methanol (1200 ppm), ethanol (1200 ppm), IPA (2400 ppm), TBA (2400 ppm), and 2,4 DMP (1200 ppm). The activated carbon, however, was not used as a sorbent for PO_4^{3-} since batch studies revealed that a substantial mass of PO_4^{3-} could be extracted from the unused samples of the media. Instead, the PSFM cartridge contained a section of activated carbon in series with the Lewatit S6328A, which was used to sorb PO_4^{3-}.

Cartridges (L = 14 cm, I.D. = 1.5 cm) were packed so the last 57±5% was filled with the activated carbon/tracer combination; the remaining 43±5% was packed with Lewatit resin to sorb PO_4^{3-} (Figure 3-3). Lewatit was placed up-gradient of the activated carbon so that no tracers would sorb to the resin upon elution, which could interfere with PO_4^{3-} analysis. This combination of media types was packed into glass columns (L = 14 cm, I.D. = 1.5 cm) using techniques described in Section 2.2.2.

After deployment, the cartridges were put on ice until they could be dissected and analyzed. The cartridges were dissected by carefully separating the resin from the activated carbon. The small amount of media in the cartridges precluded use of internal replicates, therefore no homogenization was necessary before equilibration with isobutyl alcohol (IBA) for tracer extraction. Samples equilibrated for ~24 hours at a reciprocating

speed of 25 rpm, then were removed and placed in a refrigerator to settle for ~12 hours. Tracer mass remaining was analyzed by GC/FID.

Figure 3-3: Cartridge packed with Lewatit S6328A anion exchange resin and activated carbon loaded with a resident tracer.

3.4.3 Results and Conclusions

Elution experiments were performed in the laboratory on each cartridge type before being tested in flume experiments. An elution study was used to both predict tracer desorption characteristics and how long cartridges should be deployed in the flume, since the tracer must not fully elute before analysis.

Resin/tracers. The results from the elution study for the Lewatit/tracer combination exhibited an nearly linear decrease in relative mass of tracer remaining, M_R/M_I [-] over time (Figure 3-4). This linear trend in relative mass lost shows that at low flow rates, equilibrium conditions exist within the cartridge and the tracer desorbs at a rate proportional to the flow. Differences between the slopes of the four tracers became apparent after ~50 pore volumes. Because of the poor differentiation between tracers early in the study, these tracers may be better suited for longer characterizing longer PSFM deployments (i.e. 100-300 pore volumes). This study also revealed that 2E1H and 1-octanol had similar slopes and thus eluted at a similar rate, essentially yielding the same results. Since the purpose of the suite of tracers is to estimate total pore volumes over different ranges, only one of these tracers would be required in further studies if performed over a timescale similar to that used in this study.

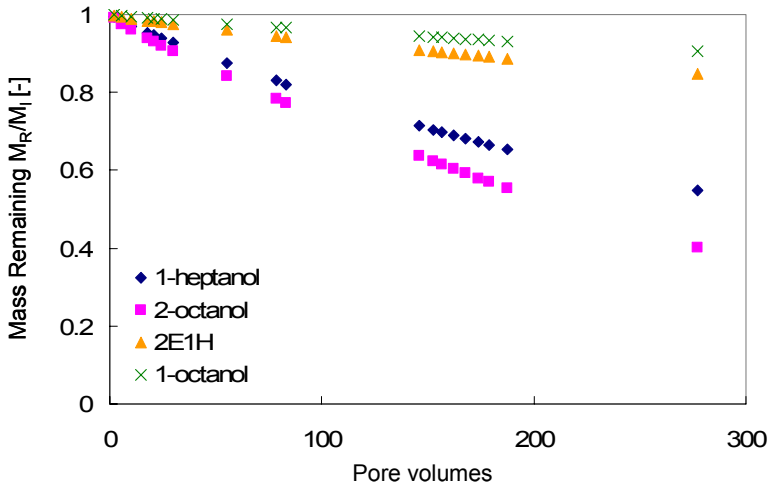

Figure 3-4: Breakthrough curves for a resin/tracer elution study at a flow rate of 0.6 mL/min.

Flume experiments were used to test performance of the PSFM body and cartridge under controlled stream flow conditions of 16 cm/s, 39 cm/s and 57 cm/s. The difference in pressure between the two ports (ΔH) were measured before cartridges were attached to the PSFM. These differences were used to estimate water velocity (v_H) using Eq. (2-4). The deployment time for the cartridges at each velocity was based on the expected mass of tracer remaining on the resin upon removal. Cartridges were allowed to flow for 20, 45 and 90 minutes, respectively. Upon analysis of the cartridge, the relative mass of tracer recovered was used to estimate the water velocity (v_T). These estimated velocities, v_H and v_T, were then compared to the true velocity as measured by the ADV.

Results showed that velocities estimated using the static port pressures correlated well to true water velocities, differing on average by only 5%. The strong correlation and small percent difference between velocities suggests that Eq. (2-4) estimated water velocity well and may be considered an appropriate equation for PSFM water flux estimation (Figure 3-5).

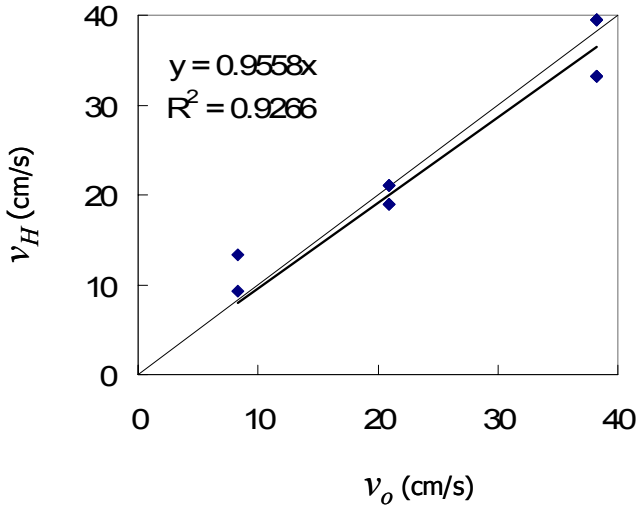

Figure 3-5: Comparison of true vs. pressure-based estimates of velocities using a cylindrical PSFM with resin/tracer cartridges.

Cartridges were analyzed to find the mass of tracer remaining on the resin after deployment. In each case, tracer analysis revealed a 100% mass recovery for all cartridges. These results are substantially different from those predicted by the elution study (Figure 3-5). Although the true reason for cartridge failure was not investigated here, it is believed that these results may be explained by non-equilibrium conditions within the cartridge. The earlier elution studies were performed at a flow rate ~10 times lower than that experienced in the flume and therefore may not properly characterize elution at higher flow rates. High flow rates through the column are a direct result of large pressure gradients across the cartridge and therefore subsequent experiments with this combination (left for future work) should investigate tracer elution at flow rates expected in the cartridge during flume experiments.

Activated carbon/tracers. Several elution studies were performed using activated carbon/tracer cartridges in order to characterize tracer elution at flow rates that may be expected under a range of stream velocities. Experiments simulating expected

flow rates through the cartridge (3.1, 5.1 and 7.1 mL/min) were performed using a constant head reservoir. Results revealed that ethanol and IPA tracers returned the most uniform elution curves for the range of flow rates tested. The elution curves of both tracers were non-linear in nature (Figure 3-6); therefore, not meeting the assumption of linear desorption required by Eq. (2-5). Therefore, these elution curves were fit with linear segments following the techniques used in Hatfield et al. (2004). The linear segments whose parameters are listed in Table 3-5, produced a linear elution function for four ranges of M_R/M_I. The mass remaining, as determined by GC analysis, was then be used to calculate Q_c based on the parameters of the linear segment which described it. The cartridge flow rate was in turn used to calculate the ΔH across the PSFM cartridge, a parameter required for estimating water velocity.

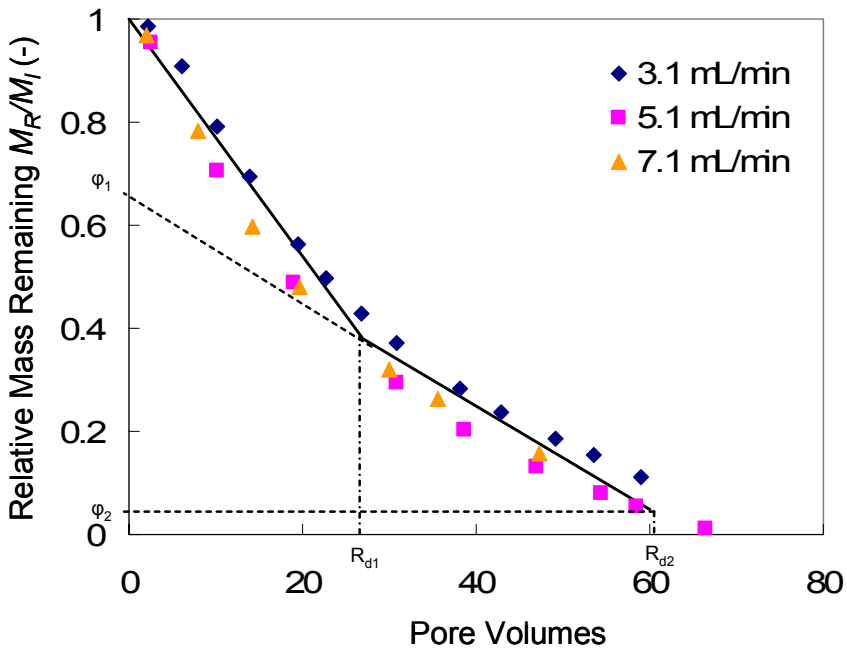

a.

Figure 3-6: Breakthrough curves for a activated carbon/tracer elution study. a) IPA elution at three different flow rates with linear segments described by the parameters φ and R_{di}.. b) Ethanol elution at three different flow rates with linear segments described by the parameters φ and R_{di}.

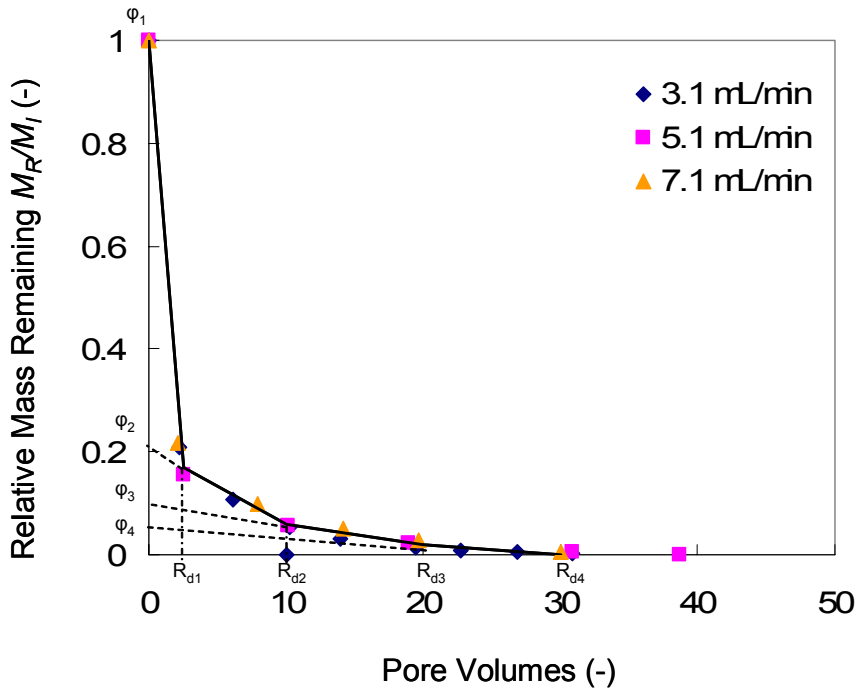

b.

Figure 3.6 Continued.

Table 3-5: Parameters used for linear segments of IPA and ethanol elution functions.

Ethanol			
φ Parameter		R_{di} Parameter	
φ_1	1.00	R_{d1}	2.50
φ_2	0.21	R_{d2}	10.00
φ_3	0.10	R_{d3}	20.00
φ_4	0.06	R_{d4}	30.00
φ_5	0.00		

Isopropyl Alcohol (IPA)			
φ Parameter		R_{di} Parameter	
φ_1	1.00	R_{d1}	27.00
φ_2	0.65	R_{d2}	60.00
φ_3	0.05		

Flume experiments were used to test the performance of the PSFM at three different velocities (24, 39, and 53 cm/s). The differences in static port pressures, ΔH, were measured before cartridges were attached to the PSFM and were used to estimate

water velocity v_H using Eq. (2-4). After ΔH measurements were recorded, the estimated velocity, v_T, was found by deploying both hydrofoil and cylindrical PSFMs. The duration of deployment was recorded and the cartridges attached to either device were analyzed for the mass of tracer remaining. The proper R_d was then found according to the relative mass remaining and was then used to calculate the average flow rate through the cartridge (Eq. 2-5). From the flow rate, the average ΔH was estimated using Eq. (2-7), which was then used to solve for the estimated water velocity (Eq. 2-4). These estimated velocities were then compared to the true velocity (v_o) as measured by the ADV.

The velocities estimated using the static pressures at the port openings (v_H) were correlated to true water velocities and differed on average by 14%. The good correlation and relatively small difference in estimated vs. true velocities verified that Eq. (2-4) is an appropriate equation for estimating water velocity using this technique (Figure 3-7).

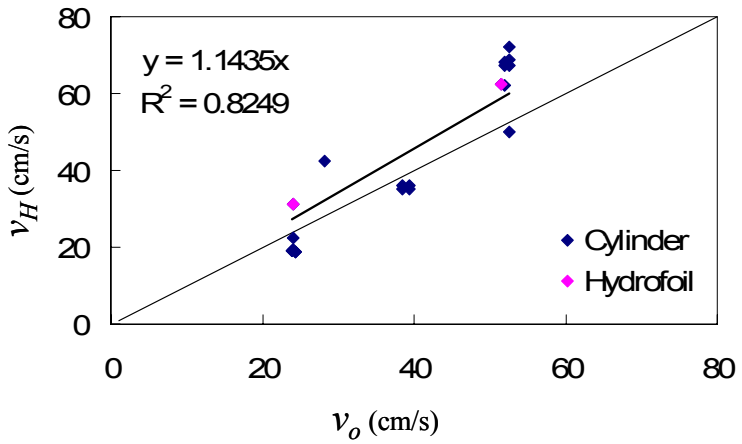

Figure 3-7: True vs. pressure-based estimate of water velocity.

Tracer-based estimates of water velocity were made using the ethanol tracer (Figure 3-8). Although the IPA tracer better characterized the total pore volumes flushed during the experiment, it could not be used for analysis. Interference from the desorption of IPA from the Lewatit S6328A resin, which had been pre-treated in IPA to remove

impurities before packing obscured true tracer information in several cartridges. Instead, the ethanol tracer was successfully used to calculate water flux, despite its short residence time in the cartridge.

The water velocities estimated from organic tracer elution yielded results that were relatively similar to the measured, true velocities. Although the correlation between tracer-estimated and true velocities was lower than the estimates made using only the static pressure differences, measurements predicted flux reasonably well, over-estimating true water velocity by 25%.

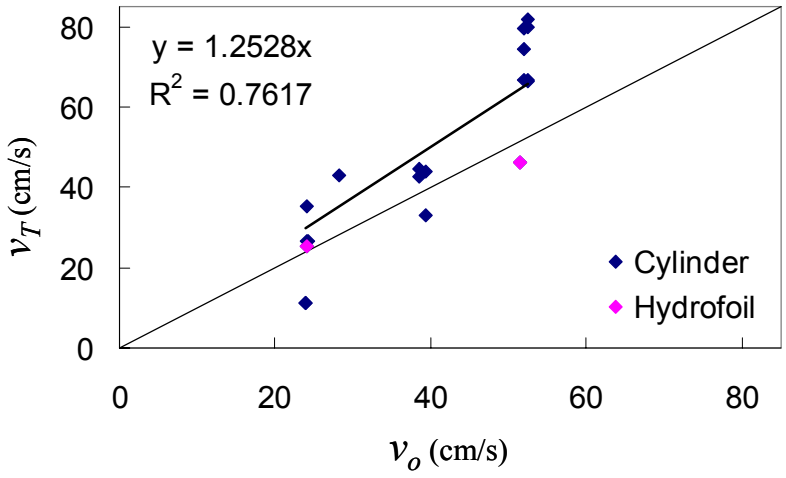

Figure 3-8: True vs. tracer-based estimate of water velocity.

Variation in both sets of estimated velocities was noticeable at higher water velocities. Over-estimation was possibly due to sorption of some of the resident tracer to the ion exchange resin before or after deployment, since no inert buffering material was used between the two medias. Variations in the estimated velocities could also be due to the temperature at which these experiments took place. Laboratory elution studies were performed under room-temperature conditions, whereas flume experiments were performed using water averaging approximately 80-85 degrees Fahrenheit; a by-product

of recirculating water through a large pump. This higher temperature may have altered the desorption properties of the resident tracers, adding error to the estimates made with these cartridges.

Although more variation was found in the activated carbon/tracer results (Figures 3-7 and 3-8) than in the resin/tracer experiment, the good elution data suggests that problems with water flux measurements were a product of experimental error, rather than chemical or design failures. Based on these data, it was concluded that this combination was best-suited for measuring water fluxes with PSFMs , needing only minor modifications to reduce errors associated with deployment.

In conclusion, it was found that velocities estimated using the difference in static pressures at two port openings most accurately predicted true water velocity. These results validated the use of the theoretical PSFM equations for determining water flux using Eq. (2-4). The dye tracer yielded close estimates of true water velocity, but the short residence time of the dye made this method of water flux estimation inappropriate for experiments that were longer in duration. Because no dye was able to accurately characterize the time frames our experiments were performed in, dye tracers were abandoned for organic tracers. Organic tracers were able to satisfy more tracer criteria than the dye tracers, but were found to estimate water velocity with less accuracy. Of the tracers tested, the resin/tracer combination elution experiment suggested these tracers may be appropriate for longer PSFM deployments under slow flow conditions, but require further study for applications at higher velocities. The activated carbon/tracer combination yielded usable elution data and the preliminary results from flume studies suggest that this method may be the best choice for future PSFM work.

CHAPTER 4
SOLUTE FLUX EXPERIMENTS

4.1 Introduction

Many studies have used ion exchange resins to measure contaminant fluxes because they strongly sorb and retain a wide range of ions (Skogley and Dobermann, 1996). In the field, resins have been successfully used to collect information on nutrient fluxes in snowmelt, soil solutions and throughfall (Susfalk and Johnson, 2002; Skogley and Dobermann, 1996; Simkin et al., 2003). In general, resins are advantageous over other types of sorbents because they are manufactured, therefore these synthetic sorbents can be made with uniform physical and chemical properties, such as particle size, ion selectivity and sorption strength (Skogley and Dobermann, 1996). For these reasons, ion exchange resins were selected as the sorbent for phosphate measurements in the PSFM cartridges.

Two kinds of ion exchange resins, Dowex Marathon MSA anion exchange resin and Lewatit S6328A anion exchange resin, were tested to evaluate their ability to sorb phosphate (PO_4^{3-}). In order to be considered an acceptable sorbent for the PSFM, the media had to meet certain criteria where 1) the sorbent must have a large capacity to tightly store the contaminant of interest and 2) the contaminant must be easy to remove from the sorbent and analyze. The resin was tested using a combination of batch, column and flume tests to fully characterize each potential porous media.

4.2 Materials and Methods

Batch experiments were performed to characterize PO_4^{3-} sorption and desorption from both Dowex Marathon MSA and Lewatit S6328A resins. All solute flux samples were analyzed using glassware washed in a 1N-HCl acid bath to remove trace contaminants. Phosphate adsorption was characterized by combining 3 g of resin with 35 mL of a solution of NaH_2PO_4 (Fisher Scientific BP329-1) dissolved in DI water. Samples represented a range of concentrations and were allowed to equilibrate for 24 hours at a reciprocating speed of 25 rpm. All samples were allowed to settle for approximately 24 hours before analysis. The amount of PO_4^{3-} adsorbed by the resin was then calculated from the amount of PO_4^{3-} left in the supernatant after equilibrium. Adsorption experiments were analyzed using the Hach Total Phosphorus Digestion Method #10127 (0-100 mg/L PO_4^{3-}) on a Hach DR/4000 Spectrophotometer (Hach, 2004).

Desorption studies were performed by replacing the supernatant from the samples used in the adsorption study with 2M KCl. Samples were allowed to equilibrate with the extraction solution for 24 hours under similar conditions. After allowing ~12 hours for settling, the supernatant of the sample was again analyzed using the same methods as described in the adsorption study.

A column experiment was performed to predict solute movement along the cartridge matrix and mass recovery percentages. The cartridge was packed using standard procedures detailed in Section 2.2.2, and connected to a constant head reservoir containing a known concentration of NaH_2PO_4 salt dissolved in DI water. The cartridges were removed before the solute was detected in the eluent to ensure that all PO_4^{3-} was retained and the porous media was sectioned and extracted using 2M KCl with techniques similar to those used in the desorption experiments. Phosphate analysis was

performed using methods and instruments similar to those described in the adsorption/desorption studies.

Following laboratory characterization, cartridges were considered ready for use in flume experiments. After estimating the volume of water in the flume, sufficient mass of NaH_2PO_4 salt was added to reach a desired solute concentration. Incidentally, the tap water used in the flume was determined to have undetectable levels of PO_4^{3-} and therefore was assumed to contribute no extra mass. In the flume, cartridges were connected to submerged PSFM bodies submerged and dissolved PO_4^{3-} was allowed to sorb to the cartridges for a recorded amount of time.

The Lewatit/tracer combination was tested at three different velocities (16, 39 and 57 cm/s) at an initial concentration C_o = 10 mg/L PO_4^{3-}. The concentration range used was high enough to ensure that sorbed PO_4^{3-} mass would be above minimum detection limits since limited access to the flume required short-duration experiments. Columns were tested at two different depths on the cylinder PSFM, both of which were expected to record the same solute and water fluxes since the velocity was found to be constant with depth in the flume (Figure 3-2). Solute mass accumulated on the column was predicted based on the initial PO_4^{3-} concentration C_o and the flow rate through the column.

The Lewatit/activated carbon combination was tested at a v = 24, 39, 53 cm/s at a C_o = 13, 15, 10 mg/L, respectively. Columns were tested both on the hydrofoil and cylindrical PSFMs at two and three depths, respectively. Since the velocity is held constant with depth in the flume, measurements occurring at the same time but at different depths were assumed to have recorded the same solute and water fluxes. Solute

mass retained was estimated in the same way PO_4^{3-} concentration was predicted in the resin/tracer trial.

Upon removal from the flow field, the cartridges were put on ice until they could be dissected and analyzed. All cartridge types were divided by their respective media type and each thoroughly mixed to ensure homogeneity. All-resin cartridges were then divided so that half the resin was analyzed for PO_4^{3-}, while the other half was analyzed for tracers. The activated carbon/resin cartridges were separated and the resin was analyzed for PO_4^{3-}. All dilutions and standards were made using tap water from the flume in order to account for any other factors that may have affected PO_4^{3-} analysis. The small amount of media in all the cartridges precluded use of internal replicates.

4.3 Results and Conclusions

Adsorptions isotherms were created based on sample concentrations ranging between 0 and 30 mg/L PO_4^{3-}. Isotherms were made for both Lewatit S6238A and Dowex Marathon MSA resins and results revealed a linear trend for both resin types. The Lewatit S6328A was found to have a K_d=1.06 L/g and an R=1800 (Figure 4-1a) and the Dowex Marathon MSA showed a K_d =1.34 L/g and an R=2200 (Figure 4-1b).

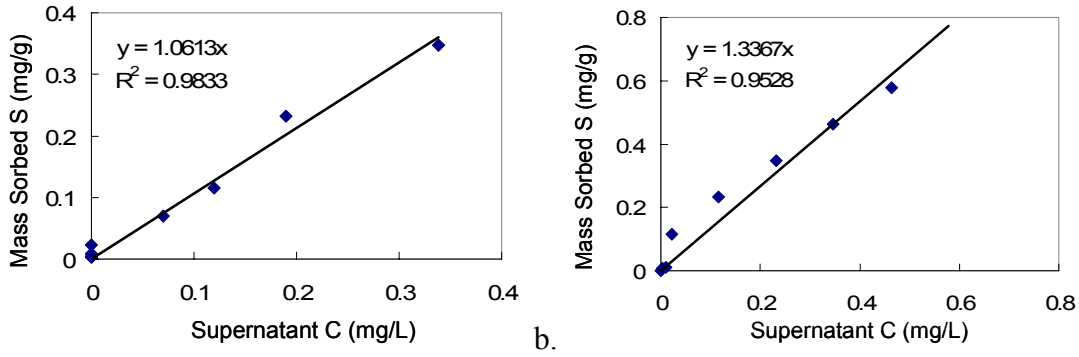

a. b.

Figure 4-1: Adsorption Isotherms for a) Lewatit S6328A and b) Dowex Marathon MSA.

The desorption studies performed on these resins revealed an extraction efficiency of 84% for the Lewatit S6328A and 85% for the Dowex Marathon MSA (Figure 4-2). Based on these data, both resins were considered to sorb and desorb PO_4^{3-} equally well.

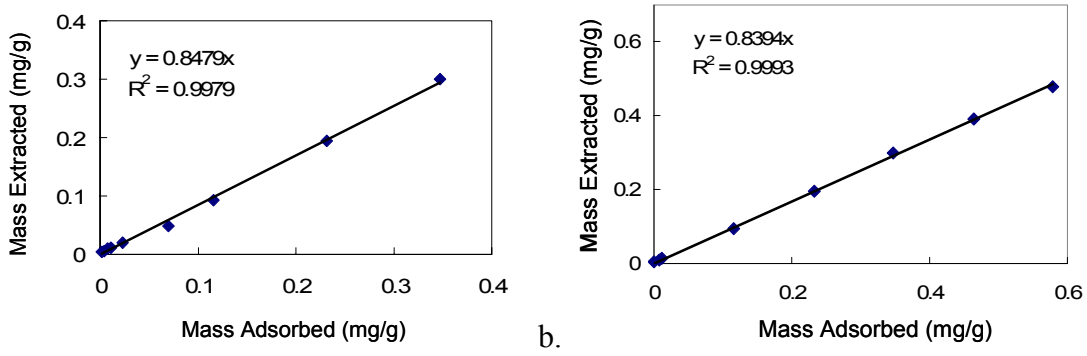

a. b.

Figure 4-2: Desorption data for a) Lewatit S6328A and b) Dowex Marathon MSA resin.

4.3.1 Column Experiments

A column experiment was performed to predict PO_4^{3-} movement under simulated flow conditions. A cartridge packed with Dowex Marathon MSA (procedures found in Section 2.2.2) was exposed to a solution containing 18 mg/L PO_4^{3-} at a flow rate of approximately 4 mL/min for two hours. Upon removal, the resin from the cartridge was divided into 8 sections and PO_4^{3-} was extracted from each section using 2M KCl. Colorimetric analysis of PO_4^{3-} was performed using methods developed by Hach (2004) and results revealed a 92% mass recovery. In addition, analysis of each section showed that after two hours, the majority of the PO_4^{3-} traveled less than 2 cm into the cartridge before sorbing to the Dowex Marathon MSA resin (Figure 4-3). No column study was performed on the Lewatit resin, since the adsorption/desorption profiles were similar.

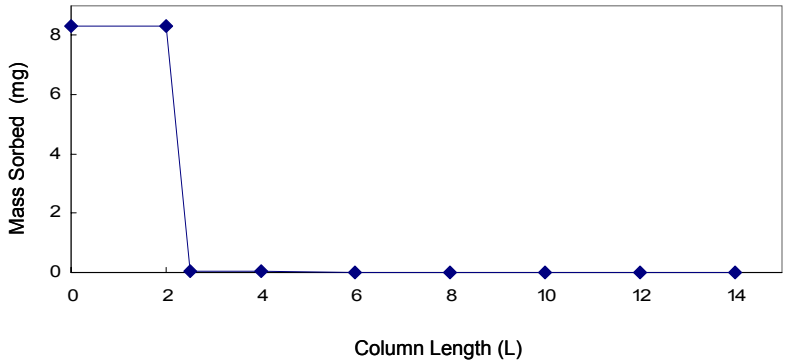

Figure 4-3: Mass sorbed with distance along a PSFM cartridge. A line is super-imposed to connect data points.

4.3.2 Steady-State Flume Experiments

Flume solute flux experiments were performed simultaneously with water flux experiments by dissolving a known mass of NaH_2PO_4 in the water and allowing the solute to sorb to the resin in the cartridge. After deployment, the cartridges were removed and the resin thoroughly mixed and extracted with 2M KCl.

Solute fluxes were calculated based on the water velocities from Chapter 3 and the mass of PO_4^{3-} recovered after extraction. Two trials were performed to measure solute flux; one using Lewatit with organic tracers, and one with activated carbon/resin combination with organic resident tracers.

Resin/tracers. The Lewatit/organic tracer study (Table 4-1) revealed that when analyzed at an 85% extraction efficiency, the flux meter over-estimated the true solute concentration by only 3% at a v = 40 cm/s, but under-estimated the same concentration during the other trials (v=15 and 60 cm/s) by 45 and 15%, respectively. The 45% difference between actual and estimated mean solute concentrations was most likely exaggerated due to the fact that only a small sample set was available for that velocity range (n=2). Sample sizes this small are not able to compensate for significant variations

in the data. In addition, the estimated concentrations reflect the errors incurred when computing the estimated water flux and the errors associated solute analysis. Small errors in both estimates were possibly magnified since the estimated C is the product of these two variables.

Table 4-1: Concentrations measured from Lewatit flux meters.

Column ID	Sorbed (mg/g)	Corr. Sorbed (mg/g)	Actual C (using v_o) (mg/L)	Estimated C (using v_H) (mg/L)
Co= 10.56 mg/L PO_4^{3-}, v=60 cm/s				
1-1	0.56	0.66	13.55	15.94
1-2	0.36	0.42	8.82	10.38
1-3	0.59	0.70	14.46	17.02
1-4	0.55	0.65	9.24	10.87
1-5	0.47	0.56	8.04	9.46
1-6	0.47	0.55	7.94	9.34
Co= 9.07 mg/L PO_4^{3-}, v=40 cm/s				
2-1	0.41	0.48	9.96	11.72
2-2	0.33	0.39	8.05	9.47
2-3	0.37	0.43	7.20	8.47
2-4	0.35	0.41	6.72	7.91
Co= 8.98 mg/L PO_4^{3-}, v=15 cm/s				
3-1	0.08	0.09	1.98	2.33
3-2	0.16	0.18	7.72	9.08

STATISTICS					
60 cm/s		40 cm/s		15 cm/s	
mean (n=6)	12.17	mean (n=4)	9.39	mean (n=2)	5.71
SD	3.40	SD	1.68	SD	4.77
CV	0.28	CV	0.18	CV	0.84
% Diff	14	% Diff	3	% Diff	45

Solute flux was determined using Eq. (2-8), where v_o was the water flux measured with the ADV in Chapter 3. Because no tracer data was available (due to no net loss of tracer), estimated solute flux could only be calculated using Q_c data as determined by the

static pressure differences at the port openings. Estimated solute flux J_H, was compared to the "true" solute flux, the product of the true water velocity (v_o) and the measured C_o [M/L^3]. Figure 4-4 shows that J_H is well correlated to the true solute flux differing by only 4%. This small percent difference between true and estimated solute fluxes suggests that this PSFM method may be used for estimating solute flux when the difference in port pressures is used to solve Eqs. (2-4) and (2-8).

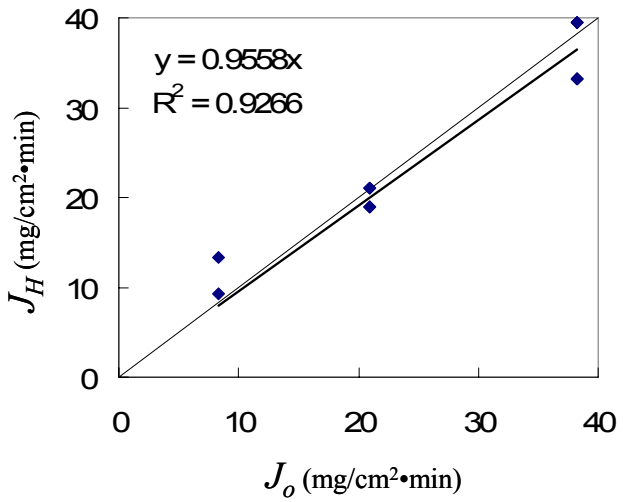

Figure 4-4: Comparison of estimated vs. true solute fluxes using a resin/tracer combination.

Activated carbon/resin. The PO_4^{3-} analysis of the cartridges in the Lewatit/activated carbon study (Table 4-2) revealed that the flux meter under-estimated the solute concentration in the flume water by 16, 52 and 43% for the velocities v= 53, 39 and 24 cm/s, respectively. This data set follows a similar trend to that found in Table 4-1, where high water velocities more accurately predicted true solute concentrations. Again, reasons for this trend may stem from the fact that higher velocities had more accurate v_o data and had a larger number of samples than either of the trials at lower velocities. Therefore, conclusions for the data in Table 4-2 are similar in nature to those given for

results shown in Table 4-1. Poor estimates of Q_c can affect estimates of C and v and small sample sizes can alter the true mean of time-averaged data, but it not clear which plays a large role in the variation of C.

Table 4-2: Concentrations measured from Lewatit/activated charcoal flux meters.

Column ID H=hydrofoil	Sorbed (mg/g)	Corr. Sorbed (mg/g)	Corr. C. (using v_o) (mg/L)	Corr. C. (using v_T) (mg/L)
v=50 cm/s, Co= 13.0 mg/L PO_4^{3-}				
1-1	0.80	0.94	12.37	14.10
1-2	0.50	0.59	12.08	10.42
1-3	0.70	0.82	11.93	14.40
1-4	0.58	0.68	12.39	10.01
1-5	0.50	0.59	12.46	8.81
1-6	0.61	0.71	12.54	10.30
1-7 (H)	0.08	0.09	12.50	
1-8 (H)	0.55	0.65	12.35	9.58
v=35 cm/s, Co= 15.0 mg/L PO_4^{3-}				
2-1	0.61	0.71	14.38	10.65
2-2	0.36	0.42	14.50	6.27
2-3	0.48	0.57	14.44	8.27
v=25 cm/s, Co= 9.8 mg/L PO_4^{3-}				
3-1	0.18	0.21	9.33	3.17
3-2	0.03	0.03	9.18	
3-3	0.13	0.15	9.61	12.79
3-4	0.10	0.12	9.66	1.56
3-5 (H)	0.13	0.15	9.63	7.07

STATISTICS

50 cm/s		35 cm/s		25 cm/s	
mean (n=8)	11.09	mean (n=3)	8.40	mean (n=5)	6.15
SD	2.22	SD	2.20	SD	4.99
CV	0.20	CV	0.26	CV	0.81
% Diff	16	% Diff	52	% Diff	43

Solute flux was determined during flume experiments using estimated water velocities v_H and v_T. Table 4-3 shows results of column performance as measured by various estimation techniques. It can be seen that for Groups 1 and 2, J_H and J_T did not differ significantly from each other, both maintaining a percent difference of ~25%. Group 3 had a large variation between mean estimated solute fluxes, due in part to cartridge malfunctions during deployment at this velocity.

Table 4-3: Differences between true and estimated solute fluxes (J_H and J_T).

STATISTICS	J_o mg/(cm^2·min)	C_{est} (mg/L)	J_H mg/(cm^2·min)	J_T mg/(cm^2·min)	J_H % Diff.	J_T % Diff.
Group 1: Co= 13.0 mg/L PO_4^{3-}, v=50 cm/s						
Mean	40.2	11.1	50.1	48.0	21.3	27.8
S.D.	0.7	2.2	5.7	11.6	10.5	17.5
C.V.	0.02	0.20	0.11	0.24	0.49	0.63
Group 2: Co= 15.0 mg/L PO_4^{3-}, v=39 cm/s						
Mean		31.8	8.4 34.1	22.7	19.1	27.4
S.D.		5.6	2.2 3.4	6.4	18.2	21.5
C.V.		0.18	0.26 0.10	0.28	0.95	0.78
Group 3: Co= 9.8 mg/L $PO4^{3-}$, v=24 cm/s						
Mean		14.1	3.3 13.5	7.1	19.6	49.5
S.D.		0.1	2.6 3.4	3.4	8.2	24.4
C.V.		0.00	0.78 0.25	0.48	0.42	0.49

Figure 4-5 compares the estimated versus true solute fluxes graphically. Pressure-based fluxes (Fig 4-5a) appeared to vary by only 17% whereas tracer-based fluxes (Fig 4-5b) both over and under-estimated solute flux by ~30% in either direction. The large differences found between J_T and J_o represents the product of smaller errors associated with estimates v_o and C. In general, J relies heavily on an accurate approximation of Q_c, since it is used to estimate both water velocity (Eq. 2-5) and water solute concentrations

(Eq. 2-9). Any small errors associated with Q_c will be incorporated into these estimates and magnified in J when using Eq. (2-8).

Despite this possible propagation of error, general positive trends were observed and suggest that there is a possibility that better correlations may be found with a larger sample set and/or modifications to the PSFM cartridges to reduce experimental error.

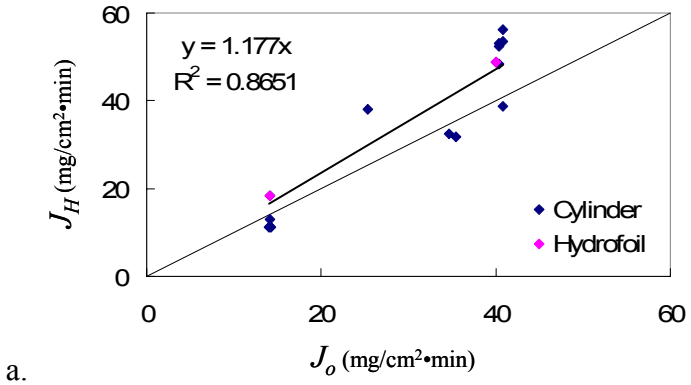

a.

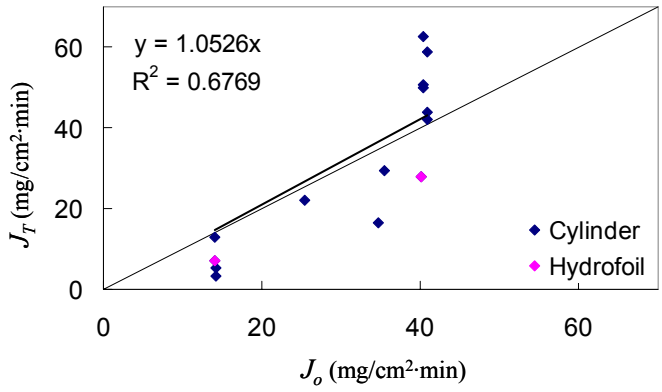

b.

Figure 4-5: Comparison of estimated vs. true solute fluxes using a resin/activated carbon combination. a) correlation between the true and predicted velocities based on Eq. (2-4). b) correlation between the true and predicted velocities based on tracer elution data.

4.3.3 Transient Flume Experiments

Transient solute flux studies were performed for all three velocities in the Lewatit/activated carbon study. In theory, solute flux as measured by the PSFM should report an average of instantaneous discrete flux measurements over time; therefore,

measurements made over a range of *C* values should be quantified by the PSFM as the average concentration over the time the cartridge was deployed.

Transient experiments were performed in the flume by attaching three cartridges to the cylindrical PSFM at an initial concentration (C_1) at t_0. At each sequential time-step, stream solute concentrations were modified by adding a known amount of $NaHPO_4$ to the flume. Mixing was considered instantaneous based on the speed with which water was recirculated in the flume. One cartridge was removed each time the solute concentration increased, thus representing the average concentration during that time step. Cartridges measured the average *C* of time periods t_0-t_1, t_0-t_2, and t_0-t_3 and were expected to show the average of the concentration changes experienced while deployed (Figure 4-6).

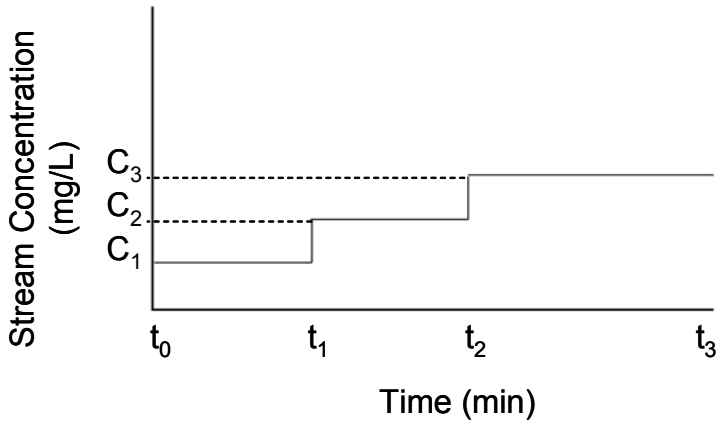

Figure 4-6: Diagram of procedures for transient solute flux experiments. C_1-C_3 represent increasing solute concentrations, where solute is added in a step-wise fashion. The x-axis represents the times at which cartridges are deployed and removed.

The flume experiment where v= 25 cm/s yielded transient solute flux data that did not accurately predict true fluxes (Table 4-4). The difference in predicted vs. estimated fluxes differed from 9-71%. These large differences in solute flux measurements are a

direct result of the large variations associated with the estimated solute concentrations and water velocities. In some cases, such as during time-step t_1-t_2, these variations are large enough to produce a solute flux measurement that appears to be accurate, but is actually the product of equal over- and underestimations of water and solute data. In addition, the fact that only one measurement was taken for each transient time/solute step means inaccuracies in data measurement (and data variation) could not be accounted for statistically.

Table 4-4: Comparison of actual (J_{ADV}) vs. transient (J_T) solute fluxes and associated parameters.

Time min	J_{ADV} mg/(cm^2·min)	J_T mg/(cm^2·min)	S.D. mg/(cm^2·min)	% Difference
t_0-t_1	34.7	16.6	12.8	70.5
t_0-t_2	46.0	41.9	2.9	9.2
t_0-t_3	55.6	35.3	14.4	44.7

Time min	C_{ADV} mg/L	C_T mg/L	S.D. mg/L	% Difference
t_0-t_1	15.00	6.27	6.2	82.2
t_0-t_2	19.92	11.98	5.6	49.7
t_0-t_3	23.52	16.92	4.7	32.7

Time min	v_{ADV} cm/s	v_T cm/s	S.D. cm/s	% Difference
t_0-t_1	38.5	42.7	2.9	10.3
t_0-t_2	38.5	54.5	11.3	34.4
t_0-t_3	39.4	33.2	4.4	17.2

Although an accurate estimation of transient solute flux was obscured by a collection of errors, distinct differences in the fluxes reported give some credibility to the theory that transient solute fluxes may be determined using the PSFM. Further studies aimed at reducing experimental error and increasing sample sizes would be needed to confirm this theory and should be investigated in the future.

CHAPTER 5
CONCLUSIONS AND IMPLICATIONS

The purpose of this research was to construct and validate the conceptual PSFM model by characterizing the device at a fundamental level. Of most importance was the ability of a physical model to validate the mathematical PSFM model as described by Klammler et al. (2004).

Two differently-shaped PSFMs were created and tested under a range of controlled stream flows to prove that the devices could generate the proper conditions required for measurement of water velocity and solute flux. Results from a comparison of the cylindrical and hydrofoil-shaped PSFMs showed that both designs were able to maintain a head gradient sufficient to accurately estimate stream velocities, validating Eq. (2-4). Although this experiment validated an important part of the PSFM theory, these experiments did not include a velocity range wide enough to fully characterize the hydraulic properties of the two devices. The range studied here was limited by the maximum velocity the flume could produce.

Cartridge development examined several possibilities for measuring stream water and solute fluxes by testing three combinations of resident tracers and porous media. The visual dye tracer showed promise early in the investigations by accurately estimating stream velocities, but failed to serve as an appropriate resident tracer for the PSFM due to short residence time within the cartridge and its possible interference with the colorimetric methods used to detect PO_4^{3-}.

Organic tracers had significantly longer residence times but were found to vary in usefulness under experimental conditions. Tracers on resins performed poorly when tested in the flume, but tracers on activated carbon estimated the difference between true and predicted stream velocities with slightly less accuracy than the visual tracers, according to the mathematics developed by Klammler et. al (2004). This reduction in accuracy is most likely a product of errors associated with construction and analysis.

Although attempts were made to reduce the uncertainty found in these results, variations in the most fundamental measurements (i.e. calculations of "true" velocities, measured pressure differences) were unavoidable. Despite these uncertainties, water velocity estimates made using resident tracer elution data and direct measurements of head differences were considered accurate enough to suggest that many of the theoretical assumptions regarding resident tracer elution and stream velocity were valid.

The accuracy solute flux estimates were less accurate than the water flux estimates, but this was most likely due low sample populations and the general propagation of errors through the analysis. Because both water and solute fluxes require an accurate estimate of Q_c, any error in the flow rate through the cartridge will be incorporated in water flux estimates and magnified in solute fluxes, due to the use of Q_c to predict both stream solute concentrations and estimated solute fluxes. In general, estimations of Q_c were often similar to the actual Q_c and solute and water flux results revealed that estimates were relatively accurate, it may be reasonable to assume that the theoretical concepts behind the device hold promise for making accurate predictions.

The transient conditions examined during solute flux experiments were at best inconclusive, thus unable to validate any of the PSFM conceptual model regarding these

estimates. This was partially due to significant error associated with the calculations, and due in part to a lack of sufficient data; one experiment with insufficient replication was not able to properly characterize the ability of the PSFM to measure transient solute fluxes.

This work opened up numerous avenues for future research. In particular, a more in-depth, proper characterization of the PSFM cartridge combinations is needed. Accurate solute and water flux ultimately relies upon the ability to correctly interpret changes in resident tracer masses. A closer examination of the resin/tracer cartridge would be extremely useful, since ideally, a PSFM cartridge should only contain one porous media. Alternatively, the separation of the activated carbon and resin into two cartridges (attached in series) may also be tested. This method may be particularly useful, since the resin cartridge could be modified to sorb different contaminants without affecting the media releasing the resident tracer. No matter the method chosen, additional verification and replication of the experiments repeated at a broader range of velocities than those detailed in this study would contribute significantly to the successful validation of the PSFM model.

Ideas for immediate modifications to improve PSFM data include developing a better casing for the PSFM cartridge, since luer lock valves often loosened, and fitting the PSFMs with new tubing to reduce air leaks during experiments. In addition, modifying the flume bed (increasing the roughness coefficient) to create a velocity profile more like those found in field conditions would be useful, and possibly better prepare the PSFM for field site testing.

LIST OF REFERENCES

Annable, M.D., Hatfield, K., Cho, J., Klammler, H., Parker B.L., Cherry J.A., Rao P.S.C., 2005. Field-scale evaluation of the passive flux meter for simultaneous measurement of groundwater and contaminant fluxes. Environ. Sci. Technol., 39 (18), 7194-7201.

Carpenter, S.R., Caraco, N.F., Correll, D.L., Howarth, R.W., Sharpley, A.N., Smith, V.H., 1998. Nonpoint pollution of surface waters with phosphorus and nitrogen. Ecol. Appl., 8 (3), 559-568.

Clark, C.J., Hatfield, K., Annable, M.D., Gupta, P., Chirenje, T., 2005. Estimation of arsenic contamination in groundwater by the passive flux meter. Environ. Forensics, 6 (1), 77-82.

Cooter, W.S., 2004. Clean Water Act assessment processes in relation to changing U.S. Environmental Protection Agency management strategies. Environ. Sci. Technol., 38 (20), 5265-5273.

Dutta, K., Bhattacharjee, S., Chaudhuri, B., Mukhopadhyay, S., 2003. Oxidative degradation of malachite green by Fenton generated hydroxyl radicals in aqueous acidic media. J. Environ. Sci. Heal. A, 38 (7), 1311-1326.

Faria, P.C.C., Orfao, J.J.M., Pereira, M.F.R., 2004. Adsorption of anionic and cationic dyes on activated carbons with different surface chemistries. Water Res., 38 (8), 2043-2052.

Florida Department of Environmental Protection (FDEP) 2004a. TMDL Report: Nutrient and Dissolved Oxygen TMDL for McKay Bay. Draft. WIBD: 1584B. Bureau of Watershed Management, Tallahassee, FL.

Florida Department of Environmental Protection (FDEP) 2004b. TMDL Report: Nutrient TMDL for Lower Sweetwater Creek. Draft. WIBD: 1570A. Bureau of Watershed Management, Tallahassee, FL.

Florida Department of Environmental Protection (FDEP) 2004c. Total Maximum Daily Load for Total Phosphorus in Lake Okeechobee, FL. Final Version. Bureau of Watershed Management, Tallahassee, FL.

Green, S.L., 1939. Hydro-and Aero-dynamics. second edition. Sir Isaac Pitman & Sons, LTD. London. pp. 60-74.

Green, F.J., 1991. The Sigma-Aldrich Handbook of Stains, Dyes and Indicators. Aldrich Chemical Company, Inc. Milwaukee, WI.

Gupta, R.E., 1989. Hydrology and Hydraulic Systems. Prentice Hall, Englewood Cliffs, NJ, pp. 227-273.

Hach, 2004. Method #10127- Molybdovanadate Method with Acid Persulfate Digestion. Hach Company. Accessed October 2005 at http://www.hach.com/fmmimghach?/CODE%3APHOSPHORUSTOT_TNT_HI7521%7C1

Hatfield, K., Rao, P.S.C., Annable, M.D., Campbell, T.J., 2002. Device and method for measuring fluid and solute fluxes in flow systems. Patent US 6,402,547 B1.

Hatfield, K., Annable, M., Cho, J., Rao, P.S.C., Klammler, H., 2004. A direct passive method for measuring water and contaminant fluxes in porous media. J. Contam. Hydrol., 75 (3-4), 155-181.

John, J.E.A., Haberman, W.L., 1980. Introduction to Fluid Mechanics. Prentice-Hall, Englewood Cliffs, NJ, pp. 493-496.

Karcher, S., Kornmuller, A., Jekel, M., 2001. Screening of commercial sorbents for the removal of reactive dyes. Dyes Pigments, 51 (2-3), 111-125.

Karcher, S., Kornmuller, A., Jekel, M., 2002. Anion exchange resins for removal of reactive dyes from textile wastewaters. Water Res., 36 (19), 4717-4724.

Kasnavia, T., Vu, D., Sabatini, D.A., 1999. Fluorescent dye and media properties affecting sorption and tracer selection. Ground Water, 37 (3), 376-381.

Kasteel, R., Vogel, H.-J., Roth, K., 2002. Effect of non-linear adsorption on the transport behavior of Brilliant Blue in a field soil. Eur. J. Soil Sci., 53 (2), 231-240.

Klammler, H., Hatfield, K., Annable, M., Jawitz, J., Padowski, J., 2004. The passive surface water flux meter to measure cumulative water and solute mass fluxes. EOS Trans., 85 (47), Fall Meet. Suppl., Abstract H13C-0422.

Krazner, K., 2005. The human context for Everglades restoration: the South Florida case study. Yale F&ES Bulletin, 107, 25-59. Accessed September 2005 at http://www.yale.edu/environment/publications/bulletin/107pdfs/107Kranzer.pdf

Meybeck, M., Helmer, R., 1989. The quality of rivers: from pristine stage to global pollution. Global Planet. Change, 75 (4), 283-309.

Morais, L.C., Freitas, O.M., Goncalves, E.P., Vasconcelos, L.T., Beca, C.G.G., 1999. Reactive dyes removal from wastewaters by adsorption on eucalyptus bark: variables that define the process. Water Res., 33 (4), 979-988.

Prabhata, K.S., 1992. Sluice-gate discharge equations. J. Irrig. Drain. E-ASCE, 118 (1), 57-60.

Parry, R., 1998. Agricultural phosphorus and water quality: A U.S. Environmental Protection Agency perspective. J. Environ. Qual., 27 (2), 258-261.

Perry, W., 2004. Elements of South Florida's comprehensive Everglades restoration plan. Ecotoxicology, 13 (3), 185-193.

Reddy, K.R., Kadlec, R.H., Flaig, E., 1999. Phosphorus retention in streams and wetlands: a review. Crit. Rev. Env. Sci. Tec., 29 (1), 83-146.

Simkin, S.M., Lewis, D.N., Weathers, K.C., Lovett, G.M., Schwarz, K., 2004. Determination of sulfate, nitrate, and chloride in throughfall using ion-exchange resins. Water Air Soil Poll., 153 (1-4), 343-354.

Skogley, E.O., Dobermann, A., 1996. Synthetic ion-exchange resins: soil and environmental studies. J. Environ. Qual., 25 (1), 13-24.

Smart, P.L., Laidlaw, I.M.S., 1977. An evaluation of some fluorescent dyes for water tracing. Water Resour. Res. 13 (1), 15-33.

Stern, D.A., Khanbilvardi, R., Alair, J.C., Richardson, W., 2001. Description of flow through a natural wetland using dye tracer tests. Ecol. Eng., 18 (2), 173-184.

Sun, Q.Y., Yang, L.Z., 2003. The adsorption of basic dyes from aqueous solution on modified peat-resin particle. Water Res., 37 (7), 1535-1544.

Susfalk, R.B., Johnson, D.W., 2002. Ion exchange resin based soil solution lysimeters and snowmelt solution collectors. Comm. Soil Sci. Plan., 33 (7-8), 1261-1275.

United States Environmental Protection Agency (USEPA), 1991. Guidance for water quality-based decisions: the TMDL process. EPA 440-4-91-001. Office of Water, Washington, D.C.

United States Environmental Protection Agency (USEPA), 1999. Protocol for developing nutrient TMDLs. EPA 841-B-99-007. Office of Water, Washington D.C.

United States Environmental Protection Agency (USEPA), 2001. Environmental Investigations Standard Operating Procedures and Quality Assurance Manual. Region 4. Athens, GA.

United States Environmental Protection Agency (USEPA), 2002a. National recommended water quality criteria: 2002. EPA 822-R-02-047. Office of Water, Washington, D.C.

United States Environmental Protection Agency (USEPA), 2002b. National water quality inventory: 2000 report. EPA 841R02001. Office of Water, Washington D.C.

United States Geological Survey (USGS), 1996. The strategy for improving water-quality monitoring in the United States---final report of the intergovernmental task force on monitoring water quality. Open-file report no. OF 95-0742. U.S. Geological Survey, Reston VA. Accessed August 2005 at http://water.usgs.gov/wicp/lopez.main.html

United States Geological Survey (USGS), 2002. The USGS role in TMDL assessments. USGS Fact Sheet FS-130-01. USGS Office of Water Quality, Reston, VA.

Wang, Q., Li, Y., Obreza, T., Munoz-Carpena, R., 2004. Monitoring stations for surface water quality. Fact Sheet SL218. University of Florida. Gainesville, FL.

Webb, W.E., Radtke, D.B., Iwatsubo, R.T., eds. 1999. Collection of water samples: U.S. Geological Survey Techniques of Water-Resources Investigations, book 9, chap. A4, accessed 23 August 2005 at http://pubs.water.usgs.gov/twri9A4/

Zdravkovich, M.M., 1997. Flow Around Circular Cylinders Vol: 1- Fundamentals. Oxford University Press, New York, NY, pp.18.

BIOGRAPHICAL SKETCH

Julie C. Padowski was born in North Tonawanda, New York in 1981. After graduating from high school, she attended the University of Rochester, NY. She graduated with a degree in environmental science (B.S.) in May 2003. In an attempt to escape the snowy North, she moved to Florida and received a Master of Science degree from the Soil and Water Science Department in December 2005. After graduation, she plans to start work in a water resources related field, hopefully remaining in a tropical or sub-tropical climate. She also plans to broaden her horizons by spending some time traveling outside the United States.